AD-A156 097 A TWO-PHASE FLOW AND HEAT TRANSFER MODEL FOR ZERO GRAVITY(U) LEVY (S) INC CAMPBELL CA D ABDOLLAHIAN ET AL. MAY 85 AFWAL-TR-85-3014 1/1

UNCLASSIFIED F/G 20/13 NL

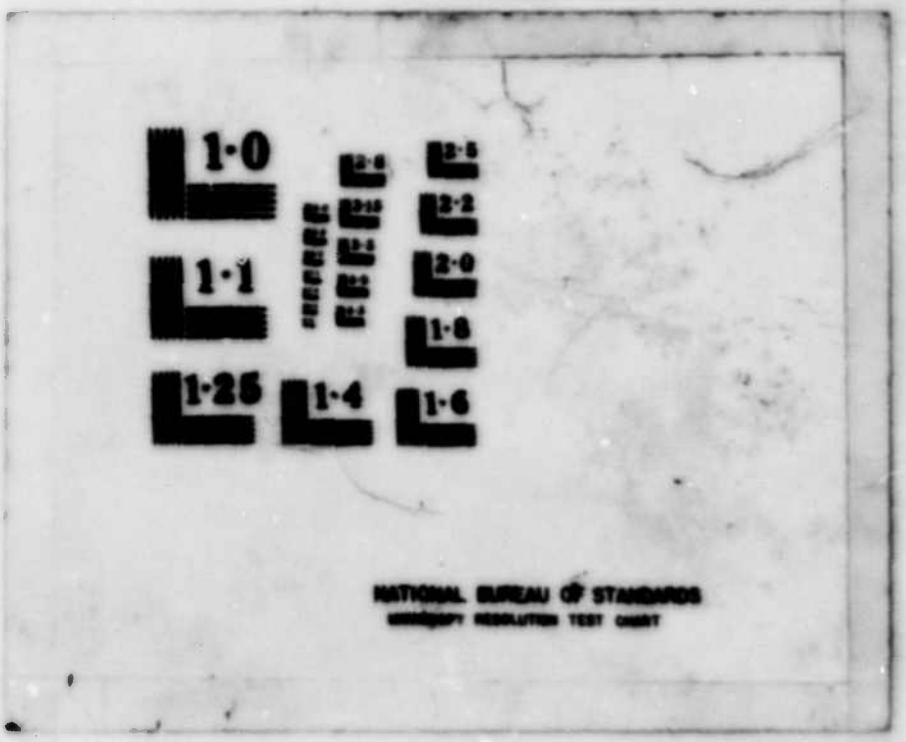
1.0
1.1
1.25
1.4
1.6
2.2
2.0
1.8
NATIONAL BUREAU OF STANDARDS

AFWAL-TR-85-3014

A TWO-PHASE FLOW AND HEAT TRANSFER MODEL FOR ZERO GRAVITY

Davood Abdollahian
Salomon Levy

S. Levy Incorporated
3425 South Bascom Ave.
Campbell, California 95008

Final Report for Period September 1984 - March 1985

May 1985

FLIGHT DYNAMICS LABORATORY
AIR FORCE WRIGHT AERONAUTICAL LABORATORIES
AIR FORCE SYSTEMS COMMAND
WRIGHT-PATTERSON AIR FORCE BASE, OHIO 45433-6553

NOTICE

When Government drawings, specifications, or other data are used for any purpose other than in connection with a definitely related Government procurement operation, the United States Government thereby incurs no responsibility nor any obligation whatsoever; and the fact that the government may have formulated, furnished, or in any way supplied the said drawings, specifications, or other data, is not to be regarded by implication or otherwise as in any manner licensing the holder or any other person or corporation, or conveying any rights or permission to manufacture use, or sell any patented invention that may in any way be related thereto.

This report has been reviewed by the Office of Public Affairs (ASD/PA) and is releasable to the National Technical Information Service (NTIS). At NTIS, it will be available to the general public, including foreign nations.

This technical report has been reviewed and is approved for publication.

William L. Haskin

WILLIAM L. HASKIN
Project Engineer

Paul D. Lindquist

PAUL D. LINDQUIST
Technical Manager

FOR THE COMMANDER

SOLOMON R. METRES
Director
Vehicle Equipment Division
Flight Dynamics Laboratory

"If your address has changed, if you wish to be removed from our mailing list, or if the addressee is no longer employed by your organization please notify AFWAL/FIEE, W-PAFB, OH 45433 to help us maintain a current mailing list".

Copies of this report should not be returned unless return is required by security considerations, contractual obligations, or notice on a specific document.

UNCLASSIFIED

SECURITY CLASSIFICATION OF THIS PAGE

REPORT DOCUMENTATION PAGE

1a. REPORT SECURITY CLASSIFICATION: UNCLASSIFIED	1b. RESTRICTIVE MARKINGS
2a. SECURITY CLASSIFICATION AUTHORITY	3. DISTRIBUTION/AVAILABILITY OF REPORT: Approved for public release: distribution unlimited
2b. DECLASSIFICATION/DOWNGRADING SCHEDULE	
4. PERFORMING ORGANIZATION REPORT NUMBER(S)	5. MONITORING ORGANIZATION REPORT NUMBER(S): AFWAL-TR-85-3014
6a. NAME OF PERFORMING ORGANIZATION: S. Levy, Inc. / 6b. OFFICE SYMBOL (If applicable)	7a. NAME OF MONITORING ORGANIZATION: Flight Dynamics Laboratory, Air Force Wright Aeronautical Labs.
6c. ADDRESS (City, State and ZIP Code): 3425 S. Bascom Ave., Campbell, CA 95008-7006	7b. ADDRESS (City, State and ZIP Code): AFWAL/FIEE, Wright-Patterson AFB, OH 45433-6553
8a. NAME OF FUNDING/SPONSORING ORGANIZATION: Flight Dynamics Lab. / 8b. OFFICE SYMBOL (If applicable): AFWAL/FIEE	9. PROCUREMENT INSTRUMENT IDENTIFICATION NUMBER: F33615-84-C-3412
8c. ADDRESS (City, State and ZIP Code): Wright-Patterson AFB, OH 45433-6553	10. SOURCE OF FUNDING NOS: PROGRAM ELEMENT NO: 65502F; PROJECT NO: 3005; TASK NO: 30; WORK UNIT NO: 10
11. TITLE (Include Security Classification): A TWO-PHASE FLOW AND HEAT TRANSFER MODEL FOR ZERO GRAVITY	
12. PERSONAL AUTHOR(S): Davood Abdollahian and Salomon Levy	
13a. TYPE OF REPORT: Final / 13b. TIME COVERED: FROM Sep 84 TO Mar 85	14. DATE OF REPORT (Yr., Mo., Day): MAY 1985 / 15. PAGE COUNT: 71
16. SUPPLEMENTARY NOTATION	

17. COSATI CODES		
FIELD	GROUP	SUB GR.
20	04	
20	13	

18. SUBJECT TERMS (Continue on reverse if necessary and identify by block number):
Two-phase flow analysis
Boiling heat transfer
Spacecraft heat transfer

19. ABSTRACT (Continue on reverse if necessary and identify by block number):

The power demands of future spacecraft are expected to grow considerably in the near future, and this will require more efficient thermal transport techniques. Due to high heat transfer coefficient, two-phase gas-liquid loops are expected to be used for removal and transport of heat to space radiators. The design of such cooling systems requires a knowledge of two-phase flow and heat transfer at reduced and zero gravities. The objective of this study was to develop or extend the earth gravity models for the two-phase friction multiplier, the void-quality relation, and the forced convective heat transfer coefficient to zero gravity situations.

Turbulent mixing length theory was used to develop a model for the two-phase fluid flow and heat transfer parameters. The velocity, density, and temperature distributions were derived by solving the conservation equations for a continuous medium and assuming equal turbulent exchanges of momentum, density, and heat. The flow was assumed to be locally homogeneous, and the void distribution was allowed to vary within the channel. The results

20. DISTRIBUTION/AVAILABILITY OF ABSTRACT: UNCLASSIFIED/UNLIMITED ☒ SAME AS RPT. ☐ DTIC USERS ☐	21. ABSTRACT SECURITY CLASSIFICATION: UNCLASSIFIED
22a. NAME OF RESPONSIBLE INDIVIDUAL: WILLIAM HASKIN	22b. TELEPHONE NUMBER (Include Area Code): (513) 255-4853 / 22c. OFFICE SYMBOL: AFWAL/FIEE

DD FORM 1473, 83 APR EDITION OF 1 JAN 73 IS OBSOLETE

UNCLASSIFIED

SECURITY CLASSIFICATION OF THIS PAGE

19.

show that the model predicts all the correct physical trends. This model contains a free parameter which should be specified from experiments at zero gravity, simulated zero gravity, or conditions where the effect of gravity can be neglected.

Additional keywords: equations; weightlessness.

PREFACE

The work described in this report was conducted as a Phase I Small Business Innovation Research (SBIR) program to begin to develop better methods for calculating two-phase fluid flow pressure gradients and heat transfer coefficients that might occur in the weightless environment of a spacecraft. More accurate analytical methods are needed to predict the in-flight performance of two-phase fluid heat transfer systems in comparison to ground test results.

The principal investigator was Dr. Davood Abdollahian with consultation from Dr. Salomon Levy. The analytical approach was based on earlier work done by the authors. This report was submitted on 22 March 1985.

Technical direction of the contract was provided by the Flight Dynamics Laboratory of the Air Force Wright Aeronautical Laboratories with Mr. William Haskin serving as project engineer.

Results of this effort are expected to be used in other SBIR contracts for further development of two-phase fluid heat transfer systems intended for spacecraft applications. The work may also provide a better understanding of basic factors affecting two-phase fluid pressure drops and temperature distributions.

TABLE OF CONTENTS

LIST OF ILLUSTRATIONS

LIST OF ILLUSTRATIONS (CONTINUED)

LIST OF TABLES

NOMENCLATURE

A	Cross Sectional Area
c	Density Distribution Parameter, Eq. 3-21
C_o	Drift Flux Distribution Parameter
C_p	Specific Heat
C, D	Constants
d	Bubble Diameter
f_o	Single Phase Liquid Friction Coefficient
F	Mixing Length Constant
F_L	Lift Force
F_σ	Surface Tension Force
G	Mass Flux
h	Heat Transfer Coefficient
H	Mixing Length Constant
K	Thermal Conductivity
K_1, K_2, K_3	Constants
ℓ_u, ℓ_ρ	Momentum and Density Mixing Lengths
Nu	Nusselt Number
P	Pressure
Pr	Prandtl Number
q	Heat Flux
Q	Dummy Integration Variable
r	Distance Measured from Tube Center
R	Tube Radius

NOMENCLATURE (CONTINUED)

Re	Reynolds Number
T	Temperature
T_m	Mixed Mean Temperature
u	Axial Velocity
v	Transverse Velocity
v_{Gj}	Drift Velocity
W	Mass Flow Rate
We	Weber Number
x	Distance in Axial Direction
X	Flow Quality
X_{tt}	Martinelli Parameter
y	Distance Measured from the Wall
Z	Parameter Defined in Eq. 3-34

Greek Letters

α	Void Fraction
ρ	Density
μ	Viscosity
τ	Shear Stress
δ	Sublayer Length
ϕ	Dissipation
ϕ_o^2	Two-Phase Friction Multiplier
Ω	Angular Velocity

NOMENCLATURE (CONTINUED)

Subscripts

a	Cross Sectional Average
c	Center Line
G	Vapor
L	Liquid
ℓ	Laminar
t	Turbulent
TP	Two-Phase
W	Wall

Superscripts

+	Non-dimensional
'	Fluctuating
- (bar)	Time Average

Section 1

INTRODUCTION

1.1 BACKGROUND

The power requirements for the future spacecrafts used in surveillance and defense missions will be increasing as they grow in sophistication and capabilities. Military spacecraft are planned to operate at power levels as high as a few hundred kilowatts in the next 20 years (1). All the surplus energy generated in the spacecraft must be transported and ultimately rejected to space. The only mode of heat transfer to space is radiation, and heat rejection is accomplished through external radiators. According to Reference (2), transport distances between the heat sources and the radiators vary from 1 to 50 meters, and transport capabilities of up to 5 million watt-meters may be needed.

The present thermal control methods are based on transport of heat via solid conductors and internal radiation, heat pipes, and single-phase liquid and gaseous loops. The components are designed for high temperature operation and large temperature variations when passive control techniques are used. Heat pipes are passive devices which can operate with small temperature differences and are also used for thermal transport in the spacecraft. When the solid conductors, internal radiation, and heat pipes cannot provide the necessary transport capability, single-phase fluid loops are employed in some spacecraft.

The high operating power of the future spacecrafts requires more effective thermal transport techniques. Two-phase flow loops can be employed for the removal and transport of heat to space radiators. With this method, the operating flow rates and temperature differences can be con-

siderably reduced and still obtain a higher heat transfer coefficient than a single-phase loop. According to Reference (2), in a typical comparison, the pump power can be reduced by two orders of magnitude and the heat transfer coefficient increased by two orders of magnitude. Nuclear power is presently being considered for multi-function communication platforms, radar surveillance, and space stations. Two-phase loops may be necessary for thermal transport in the space nuclear power systems and other high power devices.

Due to application in nuclear and chemical industries, research in two-phase flow has been in progress for over four decades. Even though it is a very complicated area, the knowledge in two-phase flow and heat transfer has been greatly advanced in the last two decades. Almost all the work in this field has been for earth gravity application and very little has been done for reduced gravity. Lack of knowledge of two-phase behavior at reduced gravities has prevented its use in space applications. However, there has been considerable research on bubble growth and pool boiling which can be used for two-phase flow studies.

Experimental and analytical studies on two-phase flow and heat transfer have been initiated by NASA and the Air Force Office of Scientific Research. Data and conclusions from these studies are needed for design of two-phase heat transfer loops for space applications.

1.2 OBJECTIVES AND SCOPE OF EFFORT

The present project has been funded by Air Force Wright Aeronautical Laboratories as a Phase I SBIR program to study two-phase flow and heat transfer under zero gravity. The overall objective of this study was to develop or extend the earth gravity correlations for two-phase friction multiplier, void-quality relation, and the forced convective two-phase heat transfer coefficient to zero gravity. These are the major engi-

neering parameters needed for design of any two-phase loop. Generally, the void-quality relation is needed to reduce the number of dependent variables. The quality can be determined from heat input, and the overall pressure drop can be calculated by knowing the void-quality relation. The two-phase friction pressure drop is usually expressed in terms of the single-phase pressure drop for the total flow considered as liquid and a two-phase multiplier. A relation for the two-phase multiplier at reduced gravity is needed for the design of the two-phase loops. Any device which employs the high heat flux characteristic of multiphase flow for heat transfer will probably be operating under nucleate or forced convective boiling regimes. However, other flow and heat transfer regimes are also possible for such equipments as condensers and heat pipes. Evaluation of the forced convective heat transfer coefficient is essential for the design and operation of two-phase loops at reduced gravities.

The present study also consisted of two initial tasks which included a review of the literature of earth gravity two-phase flow models and reduced gravity bubble growth mechanism and pool boiling. The analysis is limited to bubbly or slug flow regimes with no nucleation at the wall. The heat transfer coefficient is therefore applicable to two-component flows, bubbly flow with small amount of vapor at the wall, or to the forced convective heat transfer regime.

Section 2

BRIEF REVIEW OF PREVIOUS EFFORTS

As mentioned in the previous section, a review of the literature on two-phase flow and heat transfer at earth and reduced gravity was made. Our survey showed that very little work has been done on understanding and modeling two-phase flow at reduced gravities. However, the areas of pool boiling and critical heat flux have been addressed considerably more. An excellent review of the literature on the effects of reduced gravity on heat transfer for studies published by 1966 is given in Reference (3). Since then, there has been more work on pool boiling, bubble growth mechanism, and critical heat flux but still very little work on two-phase flow. One reason for the lack of activity in this area is the empirical nature of multiphase flow research and the difficulty in performing such experiments in reduced gravity. Generally, the reduced gravity tests are performed in laboratory drop towers, airplane trajectory, high altitude drop tests, and tests performed in rockets and satellites. However, other methods to simulate reduced gravity conditions have been proposed (4), (5), (6), (7), (8). Reference (3) has reviewed some flow conditions at 1g where the effect of gravity is expected to be negligible. Flow velocities above which the critical heat flux becomes independent of upward (1g) or downward (-1g) flow direction have been identified.

Results of an experimental study (airplane trajectory) on pressure and temperature changes in forced convective boiling at zero gravity have been reported in Ref. (9). It has been shown that the system pressure increases and boiling oscillations damp out in zero gravity. An experimental and analytical work on the two-phase flow regimes has been carried out (10), where a Froude number criterion is introduced in the

Baker's flow map. It has been concluded that the pressure drop increases significantly as the gravity decreases. Low heat flux convective boiling at zero gravity using a drop tower facility was studied in Ref. (11) and, mainly, the bubble diameter was determined. Forced convective maximum heat flux under reduced gravity was studied in Ref. (12), where small diameter heaters were used at earth gravity to simulate large heaters at reduced g. Two correlations were suggested to be used under high and low flow rates. The effect of gravity on the critical heat flux was studied in Ref. (13), where tests were performed in a vertical test section with liquid nitrogen flowing in upward and downward directions. It was found that buoyancy effect on the critical heat flux decreased with increasing inlet velocity, pressure, and subcooling. Other two-phase flow studies have reviewed the concept of two-phase loop application for spacecraft (14) and (15).

As mentioned earlier, compared to two-phase flow, considerably more work has been done on pool boiling. By reviewing analytical and experimental efforts, Ref. (3) has concluded that the pool boiling heat flux is not influenced by the gravity, while the critical and minimum heat fluxes were found to decrease with decreasing g. However, Ref. (16) has shown that for liquid hydrogen pool boiling, heat flux is a direct function of gravity. Experiments carried out by using a magnetic field to counteract the gravitational force, (4) and (5), have arrived at the same conclusion as Ref. (3) on the effect of gravity on nucleate boiling heat transfer. Mechanism of bubble growth and departure has been the subject of many investigations (17), (18) and (6). The findings are reviewed in Ref. (2) and will not be discussed here.

Section 3

TWO-PHASE VOID DISTRIBUTION AND FRICTION MULTIPLIER

Two-phase flows obey the same laws of fluid mechanics as the single-phase flow. There are basically two methods of analysis: differential and integral. In the differential method of analysis, the desired solution is obtained by solving the differential equations which mathematically describe the flow. In the integral analysis, the form of the solution is assumed rather than calculated, and the unknown parameters are determined to satisfy the boundary conditions. Integral method has been used more frequently for modeling two-phase velocity and concentration profiles, Bankoff (19), Zuber & Findlay (20).

To obtain a mathematical model for the flow, two different approaches can be adopted. The two-phase mixture can be considered as a single fluid with its own properties, or the two phases can be considered separately and conservation equations written for each phase. In the latter case, the constitutive equations which describe the transfer of mass, momentum, and energy across the interface must be specified. In the present analysis, the differential method, with the two phases considered as a mixture, will be used. This approach was used by Levy (21) for evaluating the two-phase density distribution and pressure drop. The same approach will be used here, but the equations will be modified for zero gravity conditions and also the method will be extended to solve for two-phase heat transfer.

If we consider a bubbly mixture in zero gravity flowing in a pipe, because the ratio of surface area to volume of the bubbles is large, the drag force would be dominant, and the bubbles will be traveling with nearly the same velocity as the liquid. Due to the existence of transverse forces, the bubbles will travel very close to but not exactly

along the streamlines, and some relative velocity will exist. Therefore, the two phases can be assumed to flow in a local homogeneous state. This means that the velocity of liquid and vapor phases are equal at every radial position, but there may be a concentration gradient in the pipe cross section.

A force which is normally neglected in fluid flow analyses but is important for void distribution in zero gravity is the lift force within the shear layer. Rotation of a particle due to the presence of a velocity gradient in the fluid results in a force normal to the flow direction and tends to move the particle to the region of higher velocity. At high relative Reynolds numbers, this phenomenon is known as the Magnus effect, where the particles experience significant lift in the absence of fluid shear. This force will result in the migration of the larger bubbles toward the center of the tube in the absence of gravity.

3.1 METHOD OF ANALYSIS AND THE GOVERNING EQUATIONS

In the present analysis, the two-phase system is assumed to be a continuous medium, and the single-phase turbulent mixing length theory is used to solve for void distribution and pressure drop. This method was developed by Levy (21) and is extended here for the case of zero gravity.

In the absence of gravity, the conservation of mass and momentum for a two-phase flow in a two-dimensional channel are given by:

$$\frac{\partial}{\partial x}(\rho u) + \frac{\partial}{\partial y}(\rho v) = 0 \qquad (3\text{-}1)$$

$$\rho u \frac{\partial u}{\partial x} + \rho v \frac{\partial u}{\partial y} = - \frac{\partial p}{\partial x} + \frac{\partial}{\partial y}\left(\mu \frac{\partial u}{\partial x}\right) \qquad (3\text{-}2)$$

where x is along the flow direction and y is in the transverse direction measured from the wall.

Assuming that the turbulent flow consists of an average and a fluctuating component, i.e.,

$$u = \bar{u} + u' \qquad v = \bar{v} + v' \qquad p = \bar{p} + p' \qquad \rho = \bar{\rho} + \rho'$$

and taking the time averages of the conservation equations (3-1) and (3-2), will result in

$$\frac{\partial}{\partial x}(\bar{\rho}\bar{u}) + \frac{\partial}{\partial y}(\bar{\rho}\bar{v}) + \frac{\partial}{\partial y}(\overline{\rho' v'}) = 0 \tag{3-3}$$

$$\bar{\rho}\bar{u}\frac{\partial \bar{u}}{\partial x} + \bar{\rho}\bar{v}\frac{\partial \bar{u}}{\partial y} = -\frac{\partial \bar{p}}{\partial x} + \frac{\partial}{\partial y}\left(\mu \frac{\partial \bar{u}}{\partial y}\right) - \frac{\partial}{\partial y}(\bar{\rho}\,\overline{u'v'}) - \overline{\rho' v'}\frac{\partial \bar{u}}{\partial y} \tag{3-4}$$

In taking the time averages, the following averaging rules were used:

$$\overline{\frac{\partial F}{\partial z}} = \frac{\partial}{\partial z}(\bar{F}) \qquad \overline{\bar{F} \cdot G} = \bar{F} \cdot \bar{G} \qquad \overline{F + G} = \bar{F} + \bar{G}$$

The compressible boundary layer momentum equation is obtained by multiplying equation (3-3) by u and adding to equation (3-4). The resulting equation is

$$\frac{\partial}{\partial x}(\bar{\rho}\bar{u}^2) + \frac{\partial}{\partial y}(\bar{\rho}\bar{u}\bar{v}) = -\frac{\partial \bar{p}}{\partial x} + \frac{\partial}{\partial y}\left(\mu \frac{\partial \bar{u}}{\partial y}\right) + \frac{\partial}{\partial y}(-\bar{u}\,\overline{\rho' v'} - \bar{\rho}\,\overline{u'v'}) \tag{3-5}$$

Equation (3-5) can be written in the following form

$$\frac{\partial}{\partial x}(\bar{\rho}\,\bar{u}^2) + \frac{\partial}{\partial y}(\bar{\rho}\,\bar{u}\,\bar{v}) = -\frac{\partial \bar{p}}{\partial x} + \frac{\partial \tau}{\partial y} \tag{3-6}$$

where τ is the total shear stress which is composed of the viscous or laminar and apparent or turbulent stresses.

$$\tau = \tau_\ell + \tau_t = \left(\mu \frac{\partial \bar{u}}{\partial y}\right) - (\bar{u}\,\overline{\rho' v'} + \bar{\rho}\,\overline{u' v'}) \tag{3-7}$$

In the above equation it is assumed that the two-phase viscosity does not vary in the radial direction.

It should be noted that the compressible turbulent momentum equation in the majority of fluid mechanics literature, Schlichting (22), White (23), is given in the form which was originally developed by Van Driest (24). This form of equation is given below.

$$\bar{\rho}\,\bar{u}\frac{\partial \bar{u}}{\partial x} + \bar{\rho}\,\bar{v}\frac{\partial \bar{u}}{\partial x} = -\frac{\partial \bar{p}}{\partial x} + \frac{\partial}{\partial y}\left(\mu \frac{\partial \bar{u}}{\partial y}\right) - \frac{\partial}{\partial y}(\bar{\rho}\,\overline{u'v'}) \tag{3-8}$$

where $\overline{\rho v} = \bar{\rho}\,\bar{v} + \overline{\rho' v'}$ and the total stress would be

$$\tau = \tau_\ell + \tau_t = \mu \frac{\partial \bar{u}}{\partial y} - (\bar{\rho}\,\overline{u'v'}) \tag{3-9}$$

These equations are the same as (3-4) and (3-7) with a different definition for turbulent stress. The definition of apparent turbulent stress, eq. (3-7), is made here by comparing the turbulent momentum equation, (3-4) or (3-5), to the laminar equation. The reason for the particular

grouping in equation (3-8) is that v appears only in the form of product with ρ. However, this is not the case if a solution for the density distribution is desired when the grouping of equations (3-6) and (3-7) is more appropriate.

It is known that the temporal average $u'v'$ is negative and it is normally assumed that

$$\overline{u'v'} = -C\,\bar{u}' \cdot \bar{v}' \tag{3-10}$$

we further assume that

$$\overline{\rho'v'} = -D\,\bar{\rho}' \cdot \bar{v}' \tag{3-11}$$

Using the mixing length theory for the turbulent flow and absorbing the constants C and D into the mixing length, the fluctuating components of velocities and density can be written as

$$u' = v' = \ell_u \frac{d\bar{u}}{dy} \tag{3-12}$$

$$\rho' = \ell_\rho \frac{d\bar{\rho}}{dy} \tag{3-13}$$

It is further assumed here that the exchange of momentum and void is equal; therefore, the mixing lengths for the velocity and density distributions will be equal.

$$\ell = \ell_u = \ell_\rho$$

If the shear stress is approximated by the wall shear stress, τ_w, equation (3-9) using the definitions of equations (3-12) and (3-13) becomes

$$\tau_w = \tau = \bar{u}\,\ell^2 \left(\frac{d\bar{u}}{dy}\right)\left(\frac{d\bar{\rho}}{dy}\right) + \bar{\rho}\,\ell^2 \left(\frac{d\bar{u}}{dy}\right)^2 + \mu \frac{d\bar{u}}{dy} \qquad (3\text{-}14)$$

Using the Van Driest (27) mixing length model

$$\ell = Hy\left[1 - e^{-\frac{y}{F}}\right]^2$$

equation (3-14) becomes

$$\tau_w = H^2 y^2 \frac{d\bar{u}}{dy}\frac{d}{dy}(\bar{\rho}\bar{u})\left(1 - e^{-\frac{y}{F}}\right)^2 + \mu \frac{d\bar{u}}{dy} \qquad (3\text{-}15)$$

Since we will be concerned with the mean components, the bar will not be used in the remainder of this section. The velocity, density, and pressures, unless specified, will be the mean values.

If another relation between ρ and u is found, it can be solved simultaneously with equation (3-15) to obtain the density and velocity distributions. In order to obtain such a relation, the forces acting on the bubbles will be analyzed next.

3.2 ANALYSIS OF THE FORCES ACTING ON A BUBBLE IN ZERO GRAVITY TWO-PHASE FLOW

The forces acting on a bubble during growth and departure from a heated surface have been analyzed in References (17) and (2). These forces are buoyancy, which will not exist in zero gravity; drag; surface tension; inertia; and internal pressure. The bubble will depart if the resultant of these forces is away from the heated wall. For moderate gravities,

buoyancy dominates and causes the bubble to depart. At small and zero gravities, departure may occur for fluids where the surface tension and/or inertia forces result in a net positive force away from the heated surface.

For flow boiling, a viscous drag force in the direction of the flow will be acting on the bubbles, which will tend to detach the bubbles from the wall. For two-phase flow under zero gravity situations, internal pressure and inertia forces are negligible. Because the ratio of the surface area to volume of the bubbles is large, the drag force will be dominant and the bubbles will be traveling with almost the same velocity as the liquid (local homogeneous flow).

As mentioned earlier, there is an additional force due to the rotation of a particle which is normally neglected under earth gravity when the rotation speed is not very large. This lift force acts on a particle rotating either due to the presence of fluid shear or rotating freely in the absence of fluid shear. At high relative velocities, a rotating sphere will experience a large lift force in the absence of shear. This phemomenon, called Magnus effect (25), is acted on a rotating particle at high translational velocities like a golf or tennis ball. At small relative velocities, typical of situations expected for two-phase bubbly flow, the lift force due to free particle rotation was theoretically given by Rubinow & Keller (26) to be

$$F_L = \frac{\pi}{8} d^3 \rho \Omega u \qquad (3\text{-}16)$$

where Ω is the angular velocity which for a freely rotating particle is given by

$$\Omega = 1/2 \frac{du}{dy}$$

d is the particle diameter, and ρ is the density of the fluid around the particle.

Saffman (27) has shown that when the relative velocity between the particle and the liquid is small and the fluid Reynolds number is large, lift force due to particle rotation is less by an order of magnitude than that due to shear. The lift force due to shear is given by

$$F_L = 81.2\ \mu^{1/2}\ \rho^{1/2}\ u\ \left(\frac{du}{dy}\right)^{1/2}\ d^2 \qquad (3\text{-}17)$$

where μ is the fluid viscosity.

In zero gravity, the bubbles will be traveling almost along the streamlines. Assuming that the models developed for particle suspension is applicable to bubbles, the appropriate relation for the lift force is that given by equation (3-17). When two bubbles collide, the resulting bubble will be larger and, from equation (3-17), the lift force will grow and the bubble will move to a new equilibrium position towards the center of the tube which has a higher velocity.

The main forces acting on the bubble in the transverse direction are the surface tension force, which holds the bubble together, and the lift force. From the rules of the classical fractional analysis, the ratio of these main forces should be constant in order to have similitude between two systems.

$$\frac{F_L}{F\sigma} = \frac{20.3\ \mu^{1/2}\ \rho^{1/2}\ u\ \left(\frac{du}{dy}\right)^{1/2}\ d^2}{\pi\ \ d\ \ \sigma} = K_1\ \frac{\mu}{\sigma}^{1/2}\ \rho^{1/2}\ u\ \left(\frac{du}{dy}\right)^{1/2}\ d \qquad (3\text{-}18)$$

According to Ref. (28), the critical or breakup radius of a bubble in a shear field is given by

$$d_{Crit} = \frac{2\sigma\,(We)_{Crit}}{\mu\,(\frac{du}{dy})} \qquad (3\text{-}19)$$

It is assumed here that the bubbles coalesce to the critical size upon moving to the new radial position. Substituting (3-19) in (3-18), we will get

$$K_2 \frac{(We)_{Crit}}{\mu^{1/2}} \rho^{1/2} \frac{u}{(\frac{du}{dy})^{1/2}} = K_3 \qquad (3\text{-}20)$$

The critical We, according to Ref. (28), varies from 0.82 to 1.0 for the range of μ_G/μ_L from zero to infinity. Therefore, it can be assumed that

$$(We)_{Crit} = 1.0$$

and eq. (3-20) becomes

$$\rho \sim \frac{\mu \frac{du}{dy}}{cu^2} \qquad (3\text{-}21)$$

where c is given by

$$c = \frac{2K_1}{K_3} = \frac{40.6}{K_3}$$

Dividing both sides of the above equation by the liquid density and the numerator and denominator of the right-hand side by τ_w results in

$$\frac{\rho}{\rho_L} \sim \frac{\frac{\mu}{\tau w}\frac{du}{dy}}{\frac{\rho_L}{\tau w} cu^2} \qquad (3\text{-}22)$$

In order to meet the following boundary conditions

$$\text{at} \quad y = 0 \qquad u = 0 \qquad \rho = \rho_L \qquad \frac{du}{dy} = \frac{\tau_w}{\mu}$$

$$\text{at} \quad y = R \qquad \frac{du}{dy} = 0 \qquad \rho = \rho_c$$

equation (3-22) becomes

$$\frac{\rho}{\rho_L} = \frac{\frac{\mu}{\tau w}\frac{du}{dy}}{\frac{\rho_L}{\tau w} cu^2 + \frac{\rho_L}{\rho_L - \rho_c}} + \frac{\rho_c}{\rho_L} \qquad (3\text{-}23)$$

which is the second relation between density and velocity needed for calculating the void and velocity distribution.

3.3 NON-DIMENSIONAL EQUATIONS AND METHOD OF SOLUTION

In order to solve equations (3-15) and (3-23), they are non-dimensionalized in terms of the following variables

$$y^+ = y \frac{\sqrt{\frac{\tau w}{\rho_L}}}{\mu} \rho_L$$

$$u^+ = \frac{u}{\sqrt{\frac{\tau_w}{\rho_L}}}$$

$$\rho^+ = \frac{\rho}{\rho_L} \qquad (3\text{-}24)$$

$$F^+ = F \frac{\sqrt{\frac{\tau_w}{\rho_L}}}{\nu} \rho_L$$

$$\mu^+ = \frac{\mu}{\mu_L}$$

to get

$$\frac{du^+}{dy} = c\,(\rho^+ - \rho_c{}^+)\, u^{+2} + \frac{\rho^+ - \rho_c{}^+}{1 - \rho_c{}^+} \qquad (3\text{-}25)$$

$$\frac{d\rho^+}{dy^+} = -\frac{1}{u^+}\frac{du^+}{dy^+}\,\rho^+ + \frac{1 - \mu^+ \frac{du^+}{dy^+}}{H^2\, u^+\, y^{+2} \frac{du^+}{dy^+} \left(1 - e^{-\frac{y^+}{F^+}}\right)^2} \qquad (3\text{-}26)$$

The constants H and F^+ for single-phase flows have the following values:

$$H = 0.4 \quad \text{and} \quad F^+ = 26 \qquad (3\text{-}27)$$

It is known that these mixing length constants are independent of fluid properties and flow rate. It is therefore expected that they will be applicable to turbulent two-phase flow. It is further assumed that the two-phase viscosity can be approximated by the liquid viscosity, i.e.,

$$\mu^+ = 1$$

There are a number of relations for two-phase viscosity which can be included in the present analysis without complicating the solution. However, there is not much justification for applicability of any of these viscosity relations. Liquid viscosity, which is a good approximation for the adiabatic wall situations, is therefore used.

Equations (3-25) and (3-26) can be solved simultaneously for the two variables u^+ and ρ^+ as a function of y^+. In order to have finite solutions near the wall, equation (3-26) should be modified for laminar sublayer.

Laminar Sublayer Length

Equation (3-25) is valid for both the turbulent core and the laminar sublayer. However, within the sublayer $u^+ = y^+$ and

$$\frac{du^+}{dy^+} = 1 \tag{3-28}$$

which, if substituted in equation (3-24), results in

$$(\rho^+)_{\text{Laminar}} = \rho_c^+ + \frac{1}{cy^{+2} + \frac{1}{1-\rho_c^+}}$$

The above equation can be differentiated to get the following relation

$$\left(\frac{d\rho^+}{dy^+}\right)_{\text{Laminar}} = \frac{-2cy^+}{\left(cy^{+2} + \frac{1}{1-\rho_c^+}\right)^2} \tag{3-29}$$

At the edge of the sublayer $y^+ = \delta^+$ the state variables and their derivatives should be continuous, therefore

at $y^+ = \delta^+$

$$\rho^+_{\text{Laminar}} = \rho^+_{\text{turbulent}}$$

$$\frac{du^+}{dy^+} = 1 \qquad u^+ = \delta^+$$

$$\left(\frac{d\rho^+}{dy^+}\right)_{\text{turbulent}} = -\frac{\rho^+}{y^+} = -\frac{\rho_c^+ + \dfrac{1}{c\delta^{+2} + \dfrac{1}{1-\rho_c^+}}}{\delta^+} \tag{3-30}$$

$$\left(\frac{d\rho^+}{dy^+}\right)_{\text{Laminar}} = \frac{-2c\delta^+}{\left(c\delta^{+2} + \dfrac{1}{1-\rho_c^+}\right)^2} \tag{3-31}$$

$$\left(\frac{d\rho^+}{dy^+}\right)_{\text{turbulent}} = \left(\frac{d\rho^+}{dy^+}\right)_{\text{Laminar}}$$

Equations (3-30) and (3-31) are solved for the sublayer length.

$$\delta^+ = \sqrt{\frac{1}{2c\rho_c^+}\left[1 \pm \sqrt{\frac{1 - 9\rho_c^+}{1 - \rho_c^+}}\right] - \frac{1}{c(1 - \rho_c^+)}} \qquad (3\text{-}32)$$

The above equation has a real solution for $\rho_c^+ < 1/9$ or $\rho_c < \rho_L/9$.

Even though the two non-dimensional state variables u^+ and ρ^+ can be solved as a function of y^+ from the above equations, the results will not have much practical use unless rearranged in other forms. In order to do this, the following relations are derived.

The cross-sectional average density is given by

$$\rho_a = \frac{\int \rho dA}{A} = \frac{2\int_0^R \rho r dr}{R^2}$$

Considering that $r = R - y$ and $dr = -dy$, the above equation can be non-dimensionalized to get

$$\rho_a^+ = \frac{2}{R^{+2}} \int_0^{R^+} \rho^+ (R^+ - Q)\, dQ \qquad (3\text{-}33)$$

where Q is a dummy variable.

The average mass flux is defined as

$$G = \frac{\int \rho u dA}{A} = \frac{2\int_0^R \rho u r dr}{R^2}$$

This equation can also be non-dimensionalized as follows to calculate a new variable, Z.

$$Z = \frac{G}{\rho_L \sqrt{\frac{\tau_w}{\rho_L}}} = \frac{2}{R^{+2}} \int_0^{R^+} \rho^+ u^+ (R^+ - Q)\, dQ \qquad (3\text{-}34)$$

This two-phase Reynolds number is defined as

$$Re = \frac{G\,(2R)}{\mu} = 2\,R^+\,Z \qquad (3\text{-}35)$$

The two-phase friction multiplier is defined as

$$\phi_o^2 = \frac{-\frac{(dp)}{dx}}{-\frac{(dp)}{dx}_\ell} \qquad (3\text{-}36)$$

where the denominator in the above equation is the frictional pressure gradient if the total flow is assumed to flow as liquid, i.e.,

$$-\left(\frac{dp}{dx}\right)_\ell = f_o \frac{G^2}{4\rho_L R} \qquad (3\text{-}37)$$

where f_o is the single phase liquid friction coefficient given by the following relations:

$$f_o = \frac{64}{Re} \qquad Re < 2300$$

$$f_o = 1.84 \times 10^{-4}\, Re^{0.646} \qquad 2300 < Re < 4000 \qquad (3\text{-}38)$$

$$f_o = 0.316\ Re^{-0.25} \qquad Re > 4000$$

The wall shear is given by

$$\tau_w = -\left(\frac{dp}{dx}\right)\frac{p_r}{A} = \frac{1}{8}\phi_o^2 f_o \rho_L \left(\frac{G}{\rho_L}\right)^2$$

Therefore, two-phase friction multiplier becomes

$$\phi_o^2 = \frac{8}{Z^2 f_o} \tag{3-39}$$

The void fraction for the two-phase flow is calculated from

$$\rho = \rho_L (1 - \alpha) + \rho_G \alpha$$

$$\alpha = \frac{\rho_L - \rho}{\rho_L - \rho_G} = \frac{1 - \rho^+}{1 - \frac{\rho_G}{\rho_L}} \tag{3-40}$$

The area averaged flow quality, x_a, is obtained from the following relation for local homogeneous flow

$$x_a = \frac{W_G}{W} = \frac{W_G}{GA}$$

$$W_G = \rho_G \alpha u_G = \rho_G \alpha u$$

$$\frac{W_G}{A} = \frac{\int \alpha\, u\, \rho_G\, dA}{A} = \frac{2\rho_G \int_0^R \alpha\, u\, r dr}{R^2}$$

$$= \frac{2\rho_G \int_0^R \alpha\, u\, (R-y)\, dy}{R^2}$$

Non-dimensionalizing the equation results in

$$\frac{W_G}{A} = \frac{2\rho_G \sqrt{\frac{\tau_w}{\rho_L}}}{R^{+2}} \int_0^{R^+} \alpha\, u^+ (R^+ - Q)\, dQ \qquad (3\text{-}41)$$

Using equations (3-34) and (3-41), the flow quality is calculated as follows:

$$x_a = \frac{\frac{\rho_G}{\rho_L}}{1 - \frac{\rho_G}{\rho_L}} \frac{\int_0^{R^+} (1-\rho^+)\, u^+ (R^+ - Q)\, dQ}{\int_0^{R^+} \rho^+ u^+ (R^+ - Q)\, dQ} \qquad (3\text{-}42)$$

The cross-sectional area average void becomes

$$\alpha_a = \frac{1}{A} \int \alpha dA = \frac{1 - \rho_a^+}{1 - \frac{\rho_G}{\rho_L}}$$

We next define the following void and quality relations to absorb the effect of system pressure.

$$\alpha_a^+ = \alpha_a \left(1 - \frac{\rho_G}{\rho_L}\right)$$

$$X_a^+ = X_a \frac{1 - \frac{\rho_G}{\rho_L}}{\frac{\rho_G}{\rho_L}}$$

Therefore,

$$\alpha_a^+ = 1 - \rho_a^+ \tag{3-43}$$

$$X_a^+ = \frac{\int_0^{R^+} (1-\rho^+)\, u^+ (R^+ - Q)\, dQ}{\int_0^{R^+} \rho^+ u^+ (R^+ - Q)\, dQ} \tag{3-44}$$

Method of Solution

For a given value of the constant c:

1. A non-dimensionalized center line density, ρ_c^+, is assumed.

2. The non-dimensional sublayer length, δ^+, is calculated from equation (3-32).

3. The governing equations are integrated using equations (3-28) and (3-29) for $y^+ < \delta^+$ and equations (3-25) and (3-26) for $y^+ > \delta^+$ to calculate the state variables u^+ and ρ^+ as a function of y^+.

4. At every step, the integrals (3-33), (3-34), and (3-44) are performed to calculate ρ_a^+, Re, ϕ_0^2, α_a^+, and X_a^+ from equations

(3-35), (3-39), (3-43), and (3-44).

Therefore, for a given value of the constant c, the state variables are calculated as a function of Y^+ and ρ_c^+. In addition, because for every y^+ and ρ_c^+, there are specific Re, ρ_a^+, χ_a^+, α_a^+, and ϕ_0^2, the void fraction and two-phase friction multiplier can be expressed as a function of χ_a^+ and Re.

A computer program, ZROG, was developed to perform the above calculations. This program uses the SFODE integration algorithm which solves a system of ordinary differential equations using Adams predictor-corrector method. ZROG was written in FORTRAN, and the calculations were performed on a Compupro (with MP/M operating system) and on an IBM-PC/XT (with MS-DOS operating system). All the routines were written in double precision to reduce the round-off errors. The program GRAFIT (developed by Golden Software) was used to generate the plots. This routine only connects straight lines between points and no curve fitting is performed.

3.4 RESULTS AND DISCUSSION

The parameter c introduced in equation (3-21) is actually a proportionality constant which is a combination of the constant K_1 and the similitude ratio K_3.

$$c = \frac{2\,K_1}{K_3} = \frac{40.6}{K_3}$$

The value of c should be determined from experiments, but because it affects the length of the laminar sublayer given by equation (3-32), some order or magnitude approximation for this variable can be made.

Van Driest's (24) mixing length equation used here is actually a continuous relation which can provide an eddy diffusivity applicable all

the way to the wall. However, equations (3-25) and (3-26) are not continuous close to the wall, which makes it necessary to introduce a sublayer region, as discussed before. Because the molecular diffusivity is expected to die out for y^+ = 10 to 30, from Table 3-1, which is for ρ_c^+ = 0.1, a value of the order of 1/100 seems to be appropriate. Table 3.2 gives the sublayer length for c = 1/200 and 1/400 for different values of centerline density.

Table 3-1

δ^+ Values for ρ_c^+ = 0.1

c	1	1/10	1/100	1/200	1/400	1/1000
δ^+	1.49	4.71	14.91	21.08	29.81	47.14

Table 3-2

δ^+ Values for c = 1/200 and 1/400

ρ_c^+	0.01	0.02	0.03	0.04	0.05	0.06	0.07	0.08	0.09	0.1
c=1/200	14.51	14.91	15.34	15.83	16.36	16.97	17.68	18.52	19.59	21.08
c=1/400	20.52	21.08	21.70	22.38	23.14	24.0	25.0	26.19	27.7	29.81

Velocity and density distributions for ρ_c^+ = 0.1 and for different values of c are shown in Figures 3.1 and 3.2. The density profile be-

comes flatter for smaller c. Figures 3.3 to 3.6 show u^+ and $\rho^+/\rho_c{}^+$ for c = 1/200 and c = 1/400. As discussed in the previous section, for the given value of c, two-phase friction multiplier and void fraction can be expressed as a function of flow quality and Reynolds number. Figures 3.7 to 3.10 show $\phi_o{}^2 f_o$ and α^+ as a function of χ^+ for c = 1/200 and c = 1/400. Predictions are presented in this form to absorb the effect of system pressure and the choice of single-phase friction coefficient relation.

The two-phase friction multiplier using the single-phase friction factor selected here, equation (3-38), is shown in Figures 3.11 and 3.12. At earth gravity, the two-phase friction multiplier is expected to decrease with increasing mass flux. An opposite trend is shown in Figure 3.11 and 3.12. This is due to the fact that, even though $\phi_o{}^2 f_o$ drops with increasing mass flux, f_o given by equation (3-38) has a stronger dependence on Re which results in an increasing two-phase multiplier. For larger values of c, the two-phase multiplier may show the same trend as the earth gravity case. In any event, the true coefficient for calculating the two-phase pressure drop, as shown in equations (3-36) and (3-37) is $\phi_o{}^2 f_o$, which reduces with increasing mass flow. In Figure 3.11, the two-phase friction multiplier for Reynolds number of 3000 is larger than for Reynolds number of 5000. The reason for this trend is that the single-phase friction coefficient in the transition region between Re = 2300 and Re = 4000 goes down which results in an increasing two-phase friction multiplier. As mentioned earlier, the plotting routine used here connects the data points with straight lines. Therefore, slope changes such as the ones seen on Figures 3.2 and 3.6 around y^+=10 could have been avoided if more data points were available or a curve smoothing technique was used.

The predictions using the present model can be compared to earth gravity data. Unfortunately, the void-quality data in the majority of the two-

phase flow literature is presented either as a function of thermodynamic quality or it is reported for very low qualities. The void as a function of flow quality can be obtained from the available literature, but this requires more time. Due to project limitations, this comparison is not performed in this phase of the program. However, the two-phase friction multiplier from the present model is compared to earth gravity data. This is shown in Figure 3.13 which is reproduced from Reference (29). The two-phase friction multiplier for Re = 50,000 and c = 1/200 and 1/400 are shown as a function of flow quality. From Figures 3.7 to 3.13, it can be concluded that the parameter c does not have a significant effect on the void-quality relation, while it strongly affects the two-phase friction multiplier. Figure 3.13 also shows that the two-phase multiplier increases with increasing the parameter c and, for values of 1/200 and 1/400, the two-phase multiplier is significantly smaller than the earth gravity results. This is in contrast to conclusions of Ref. (10), where the pressure drop was shown to increase as the gravity was reduced. It is believed that the present model represents the physical phenomenon correctly, but the value of c used in the predictions may be too small. As discussed in Section 5, this model predicts an increasing void fraction approaching the homogeneous distribution and a decreasing two-phase friction coefficient, $\phi_o^2 f_o$, as Reynolds number is increased. The two-phase multiplier should be larger than, but approaching the homogeneous distribution as the Reynolds number is increased. Figure 3.13 shows that the two-phase multiplier is smaller than the homogeneous value. A larger value of c (on the order of 1/20 to 1/50) would result in a larger two-phase multiplier and a decreasing trend with increasing Reynolds number. Such values of c correspond to sublayer lengths of 5 to 10 and will not affect the void-quality relation significantly. Due to time limitations, predictions with larger values of c were not performed in this phase of the project but are recommended for the future.

Following the drift flux approach (20), the generalized void-quality model can be expressed as

$$\alpha = \frac{x}{C_o \left[x + \frac{\rho_G}{\rho_L}(1-x) \right] + \frac{\rho_G V_{Gj}}{G}} \tag{3-45}$$

where C_o is the void distribution parameter and V_{Gj} is the drift velocity. For the case of local homogeneous flow, $V_{Gj} = 0$ and

$$\alpha = \frac{x}{C_o \left[x + \frac{\rho_G}{\rho_L}(1-x) \right]} \tag{3-46}$$

C_o is usually determined from experiments, and it varies between 1.0 and 1.2 for earth gravity bubbly flow. In the present analysis, an attempt was made to find the void distribution analytically using the analysis of the forces acting on the bubbles. However, there is an unknown factor, c, which should be determined from experiments. At very high pressures, the two-phase flow at earth gravity will be nearly homogeneous. In addition, ρ_L/ρ_G decreases with increasing pressure, thereby reducing the effect of gravity on the flow. In the absence of zero gravity test results, high pressure vertical two-phase flow tests can be used to estimate the parameter c.

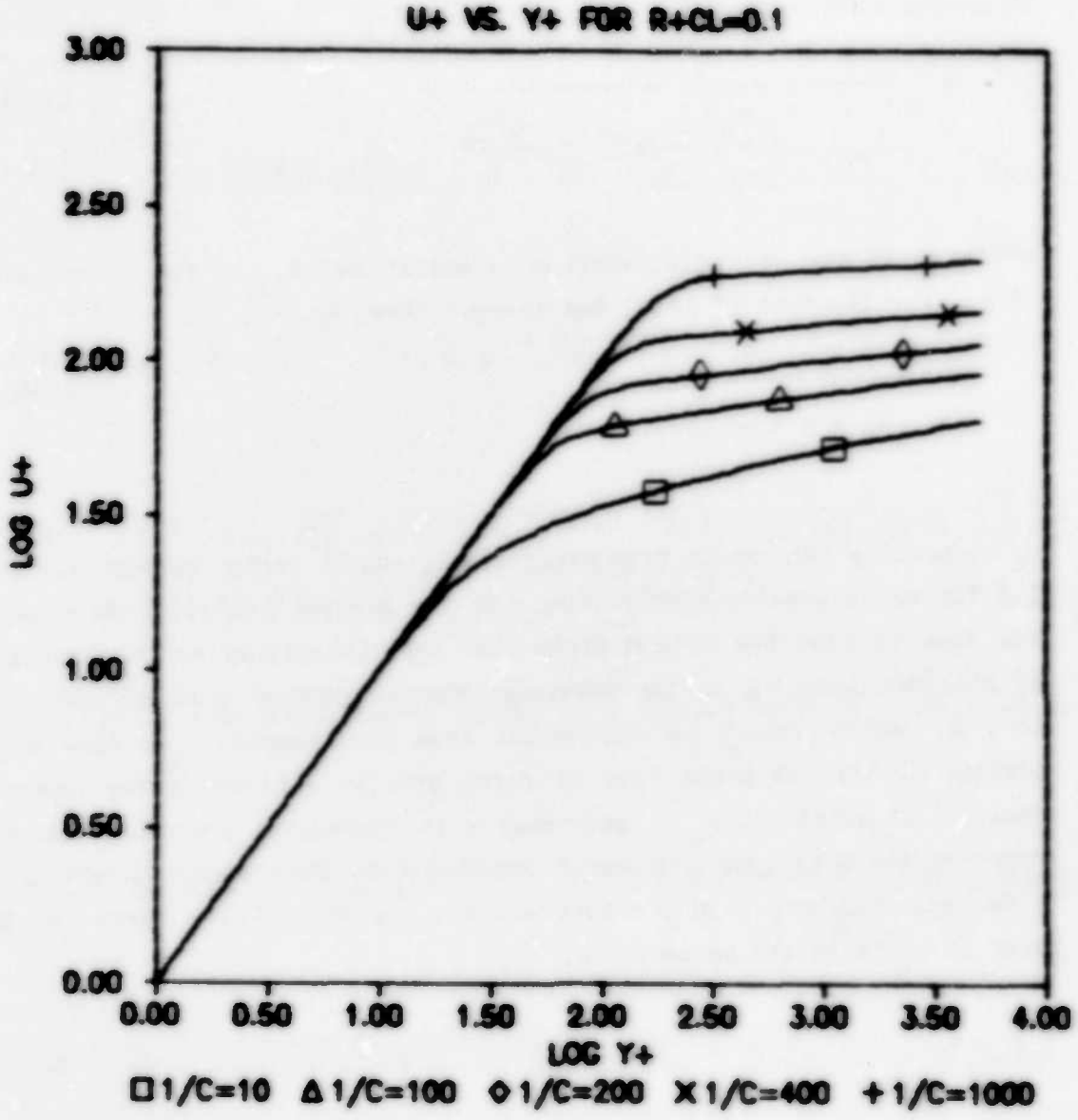

Figure 3.1. Effect of the Parameter c on the Velocity Profile for $\rho_c^+ = 0.1$

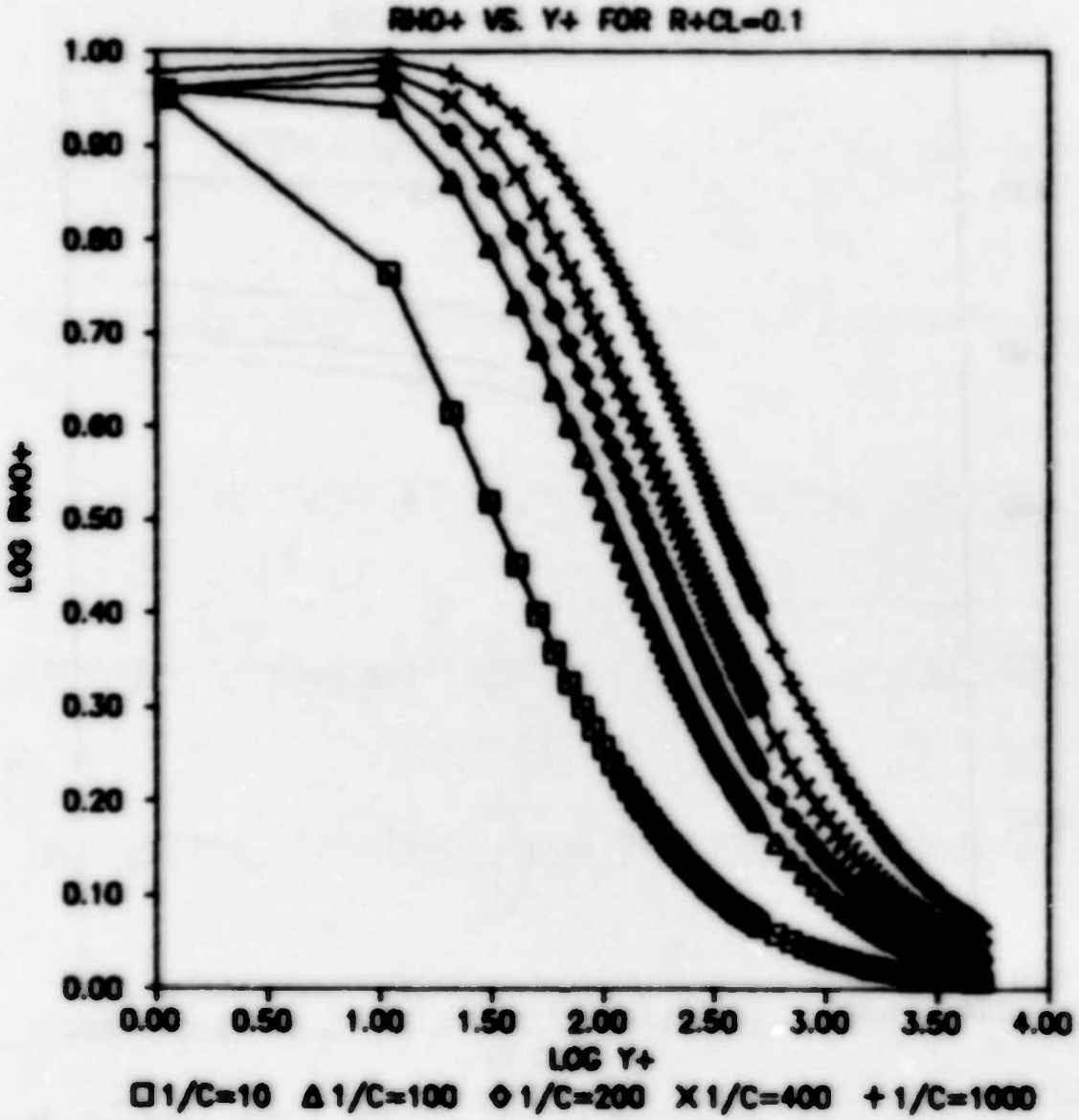

Figure 3.2. Effect of the Parameter c on the Density Profile for $\rho_c^+ = 0.1$

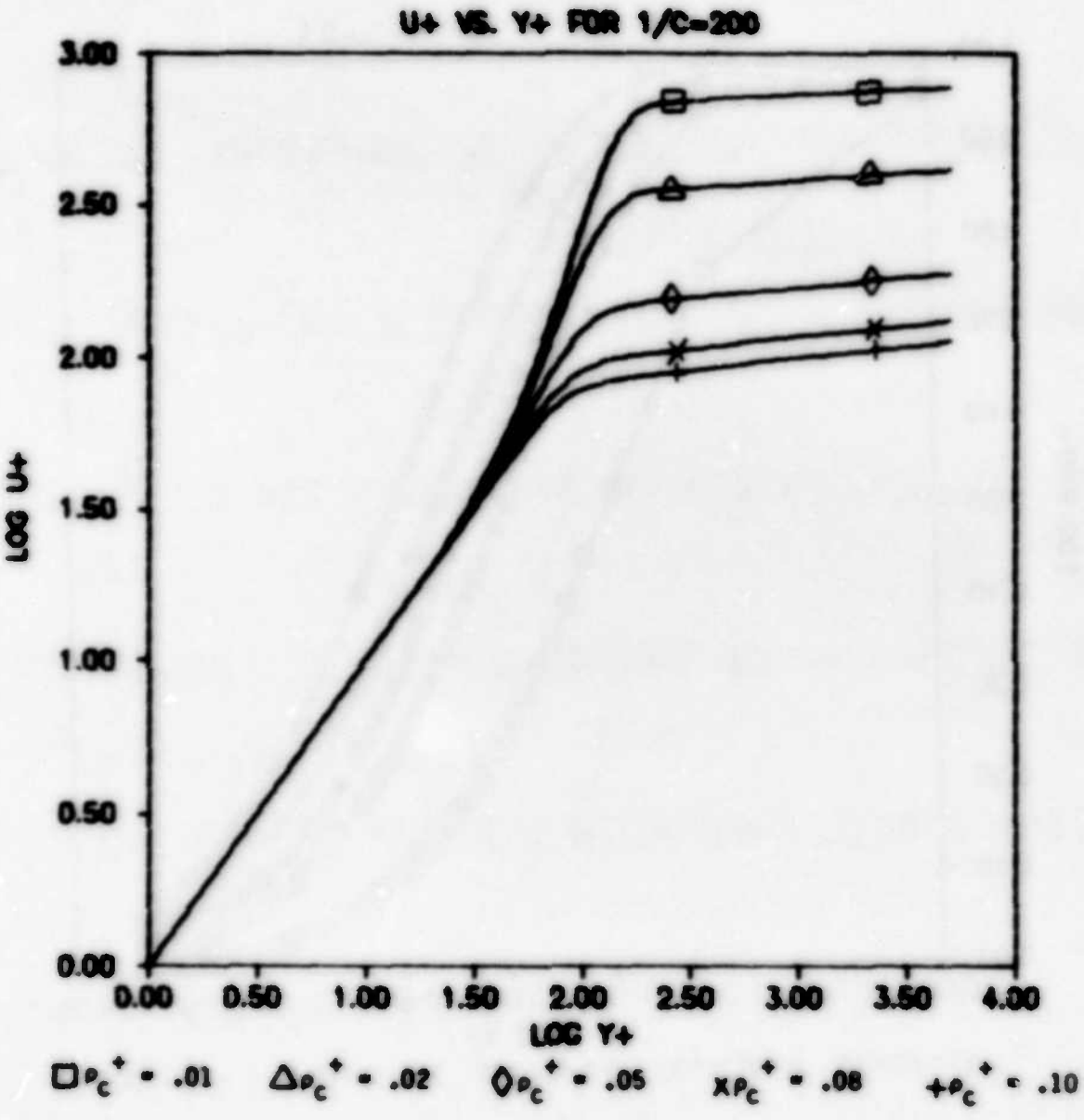

Figure 3.3. Effect of Center Line Density on Velocity Profile for C = 1/200

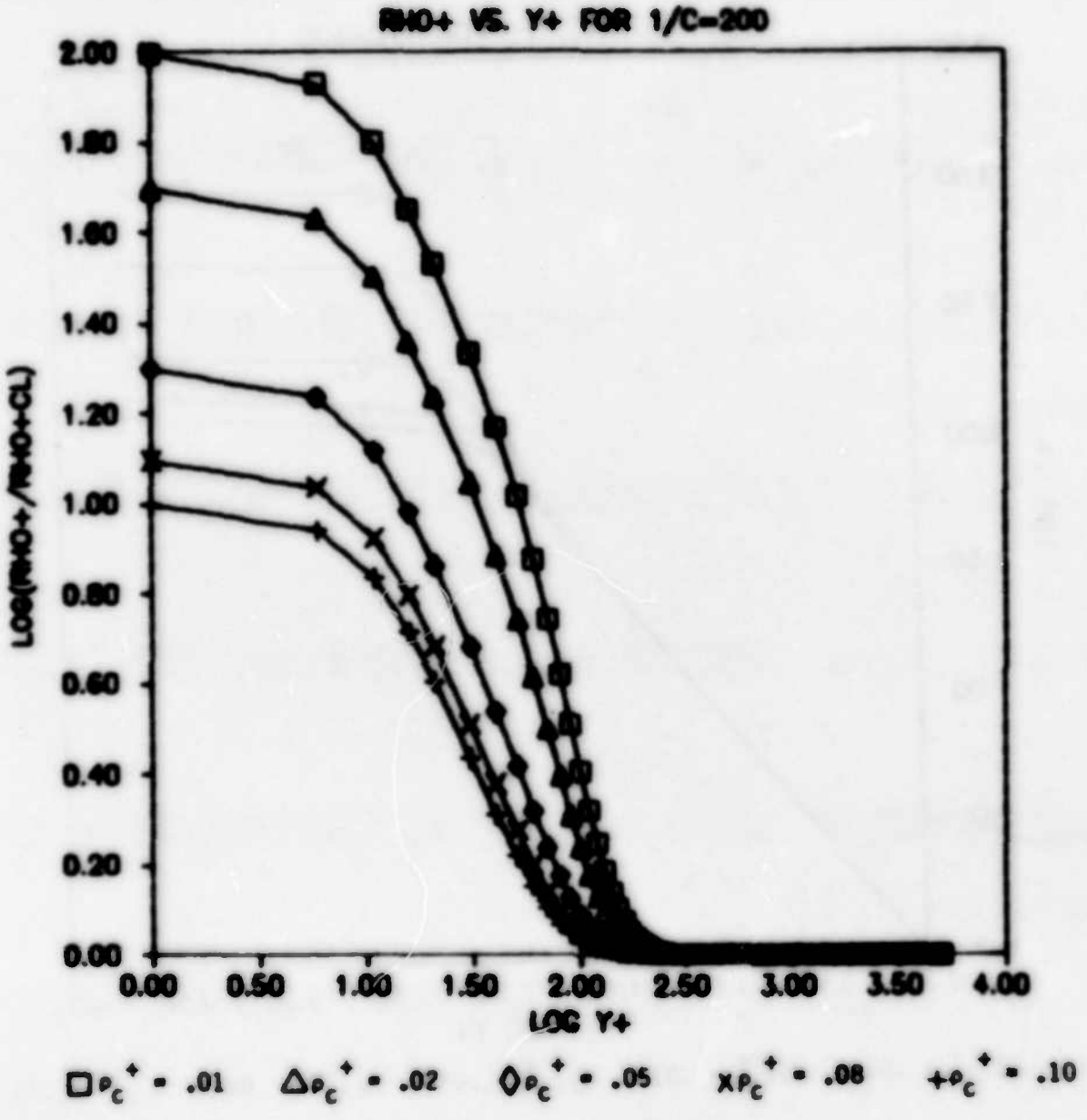

Figure 3.4. Effect of Center Line Density on Density Profile for C = 1/200

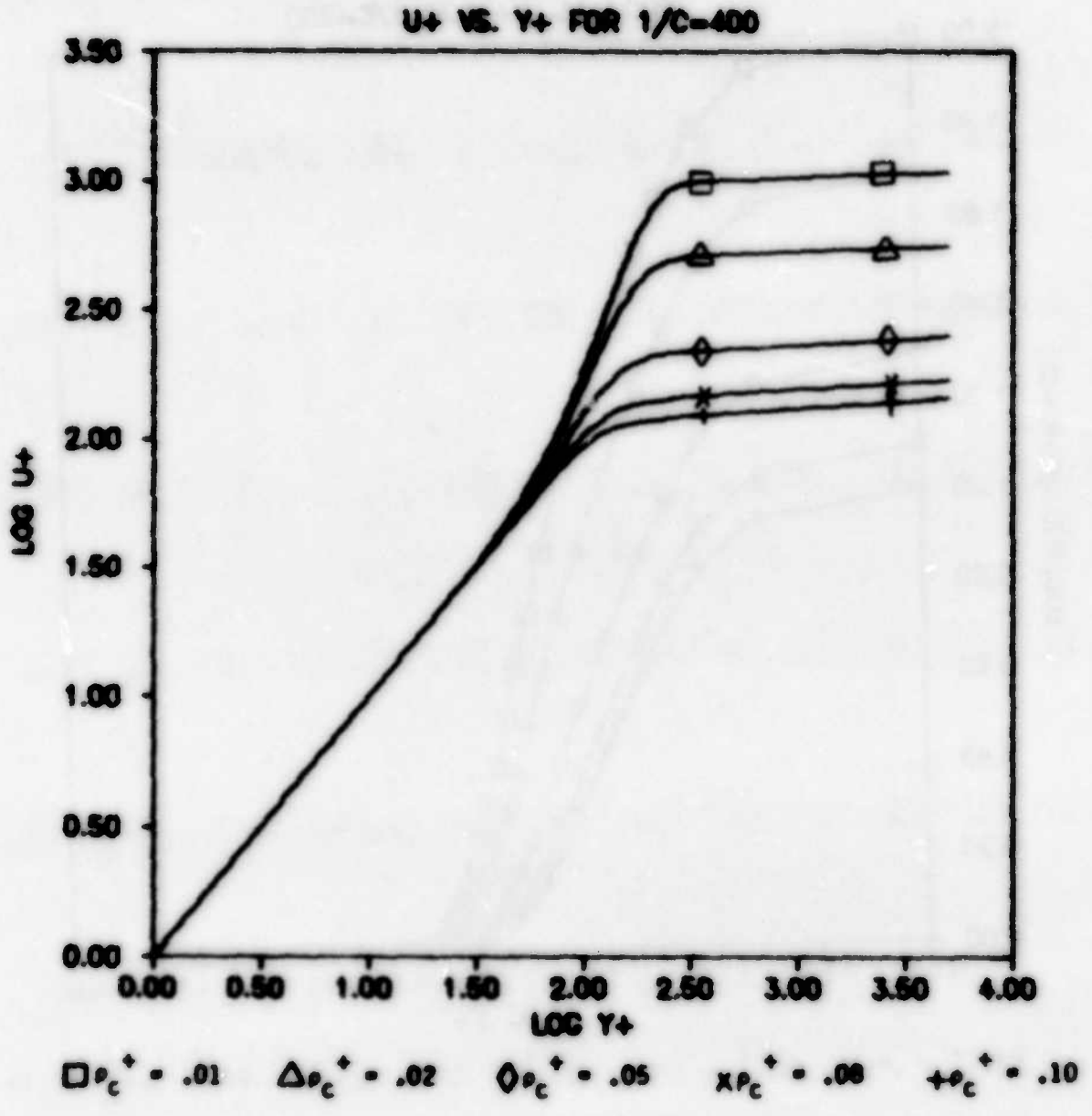

Figure 3.5. Effect of Center Line Density on Velocity Profile for C = 1/400

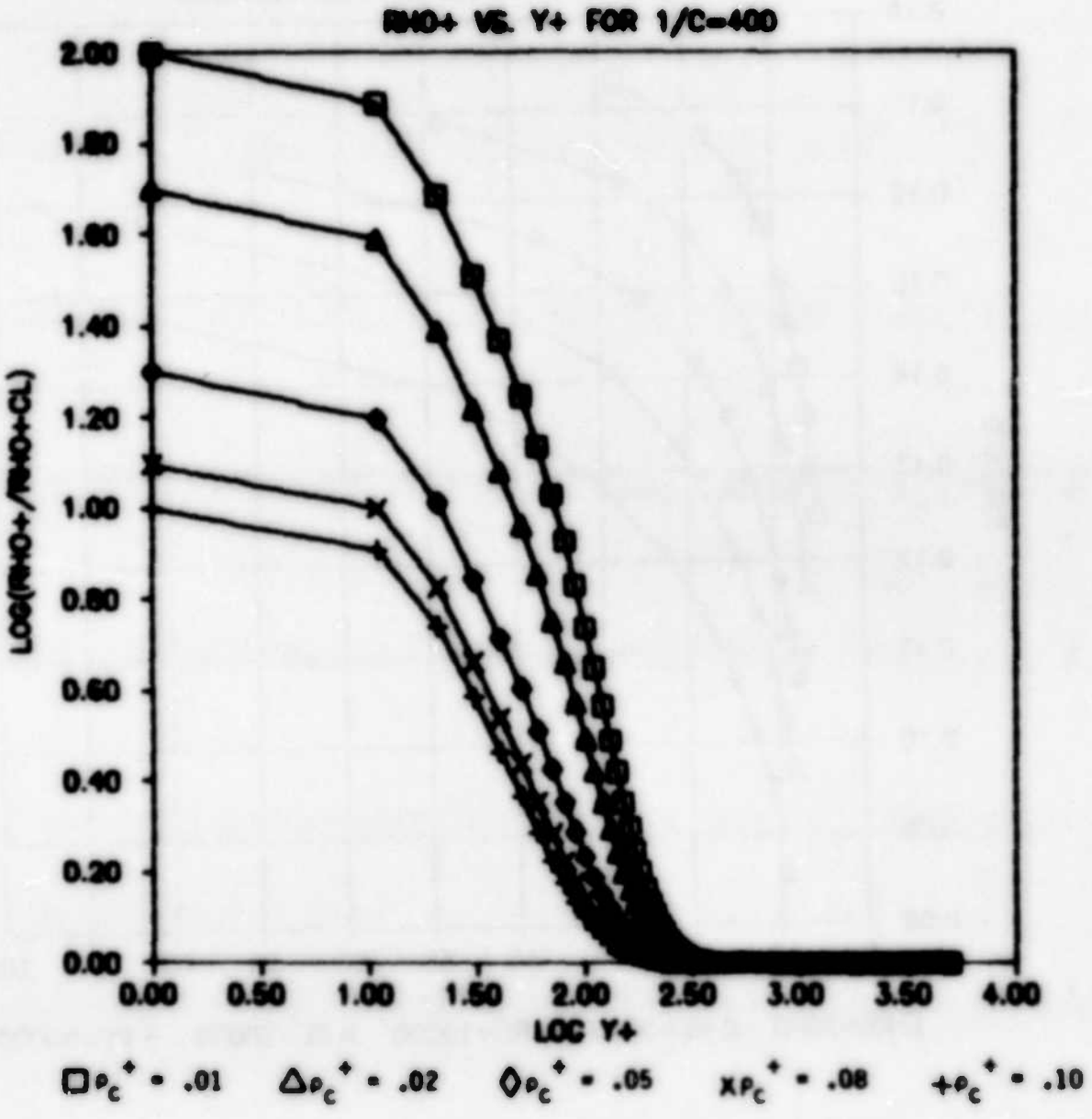

Figure 3.6. Effect of Center Line Density on Density Profile for C = 1/400

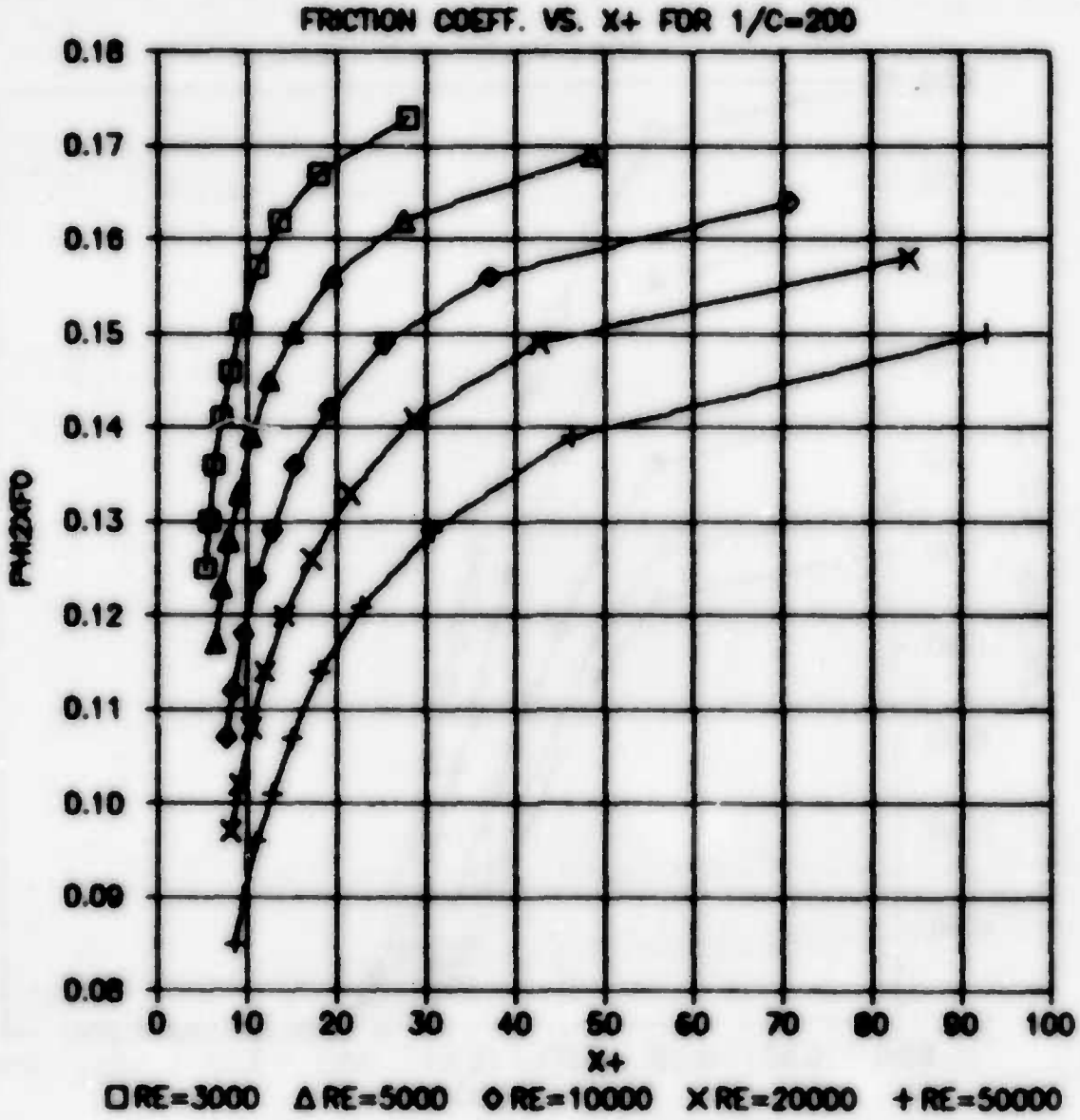

Figure 3.7. Two-Phase Friction Factor vs. Modified Flow Quality for C = 1/200

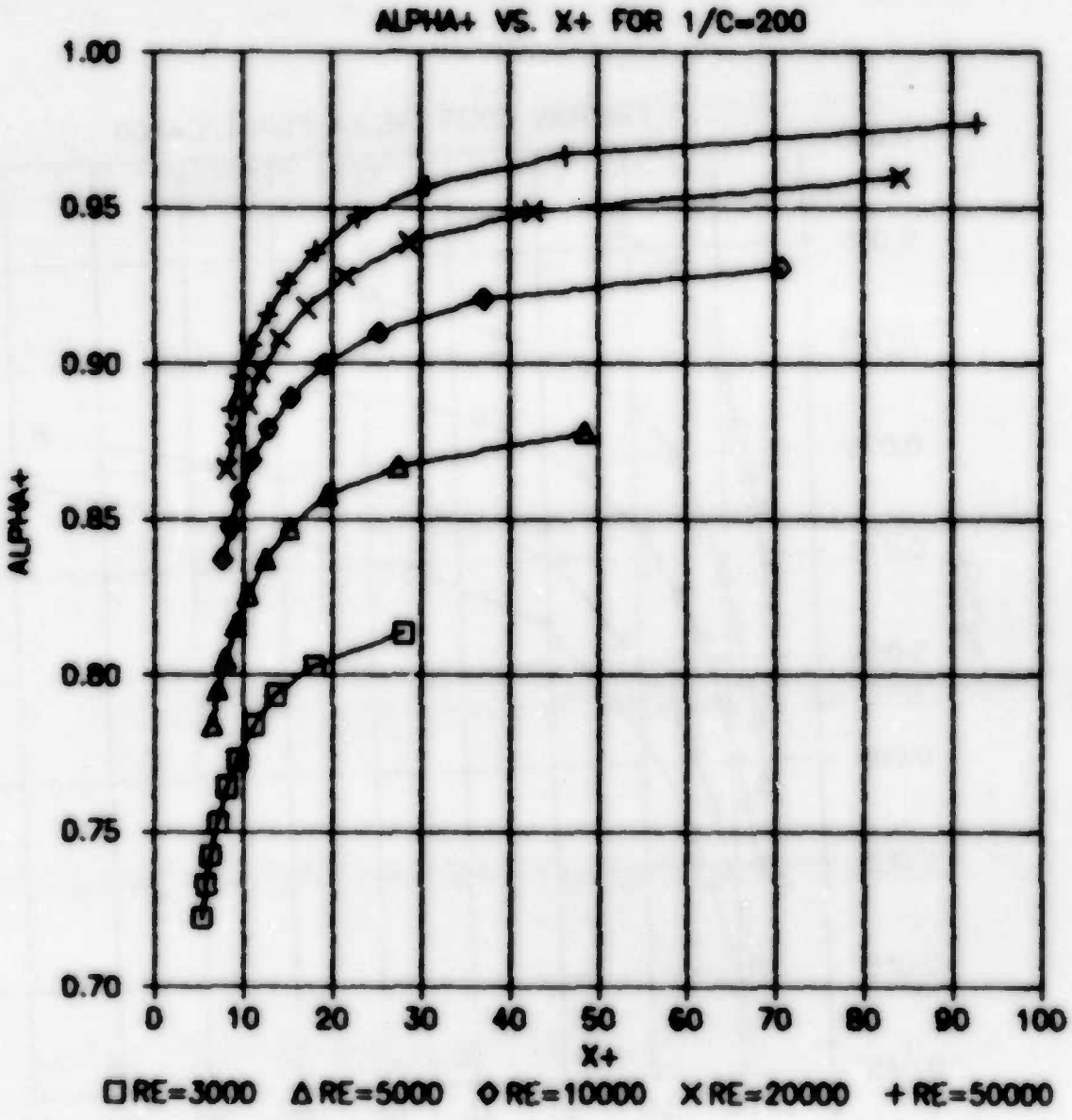

Figure 3.8. Void-Quality Profile for C = 1/200

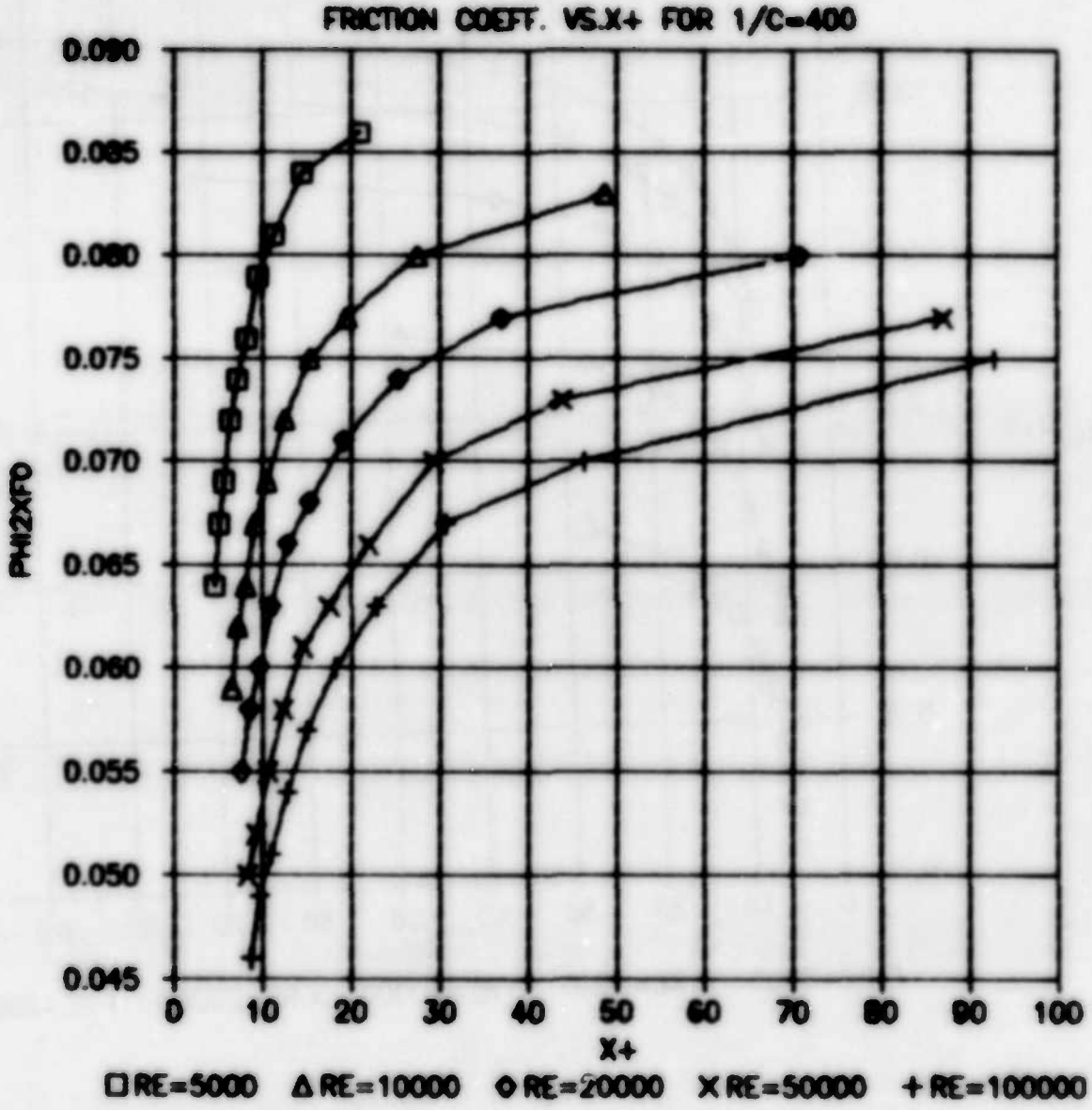

Figure 3.9. Two-Phase Friction Factor vs. Modified Flow Quality for C = 1/400

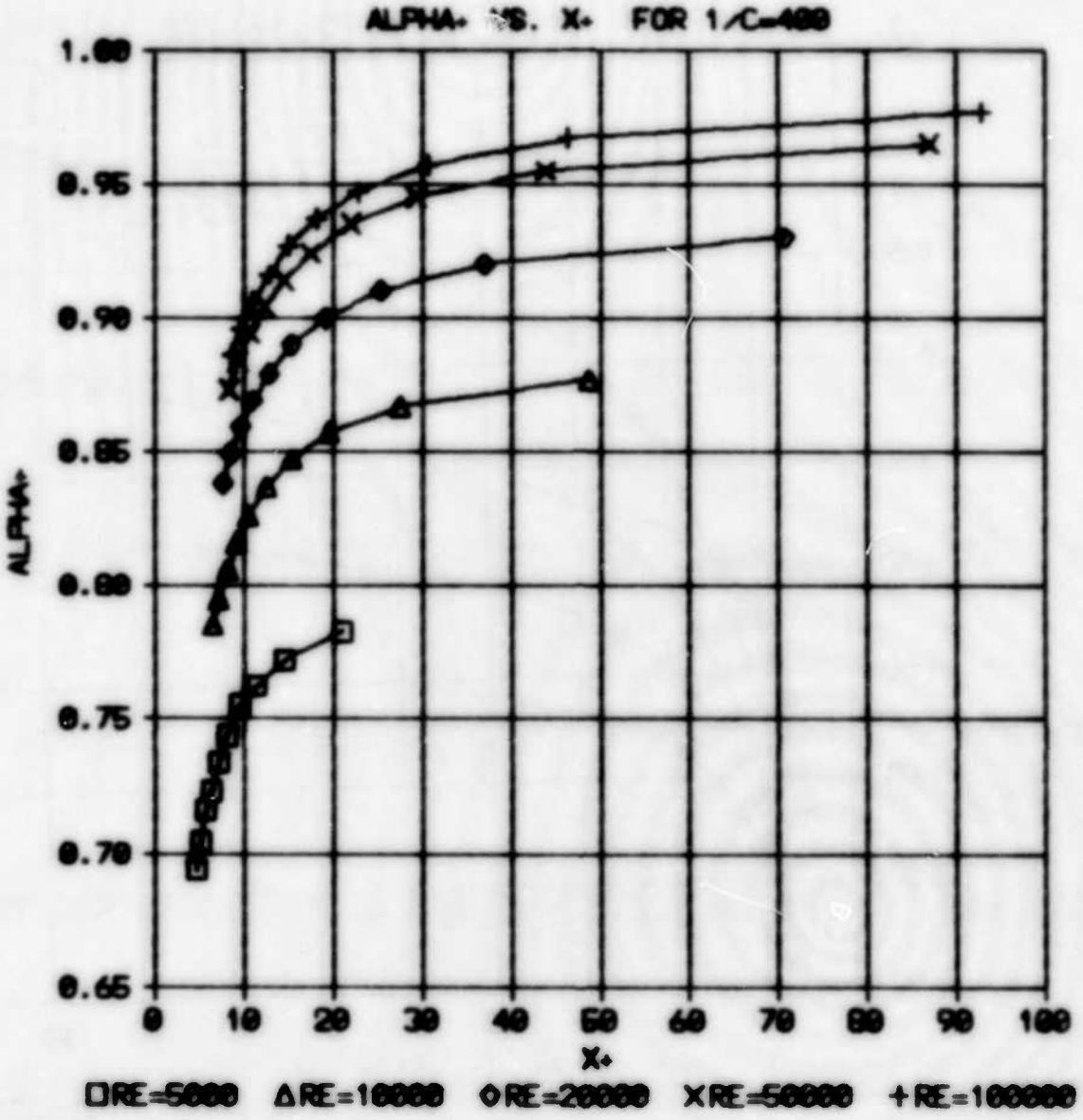

Figure 3.10. Void Quality Profile for C = 1/400

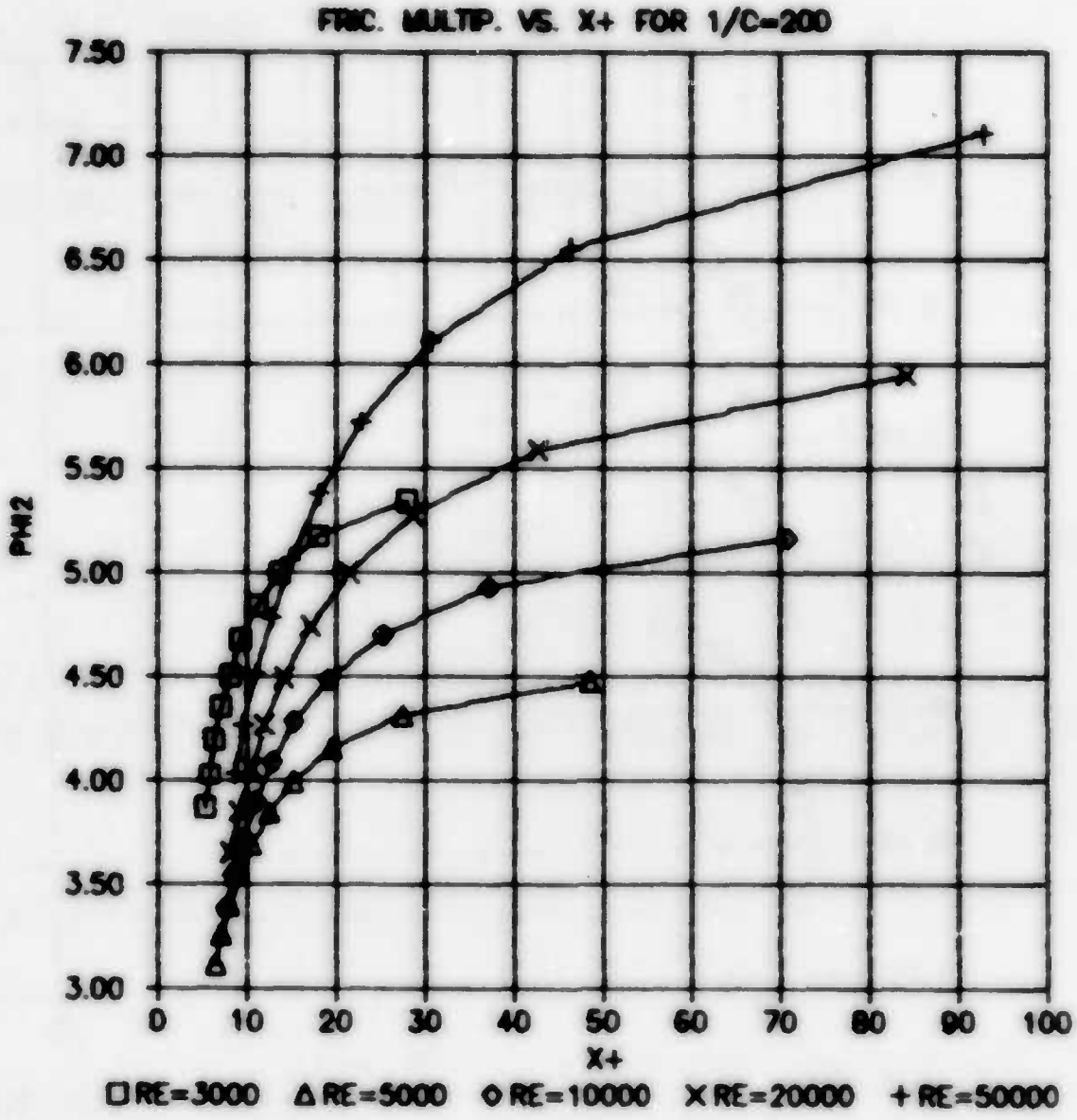

Figure 3.11. Two-Phase Friction Multiplier vs. Modified Flow Quality for C = 1/200

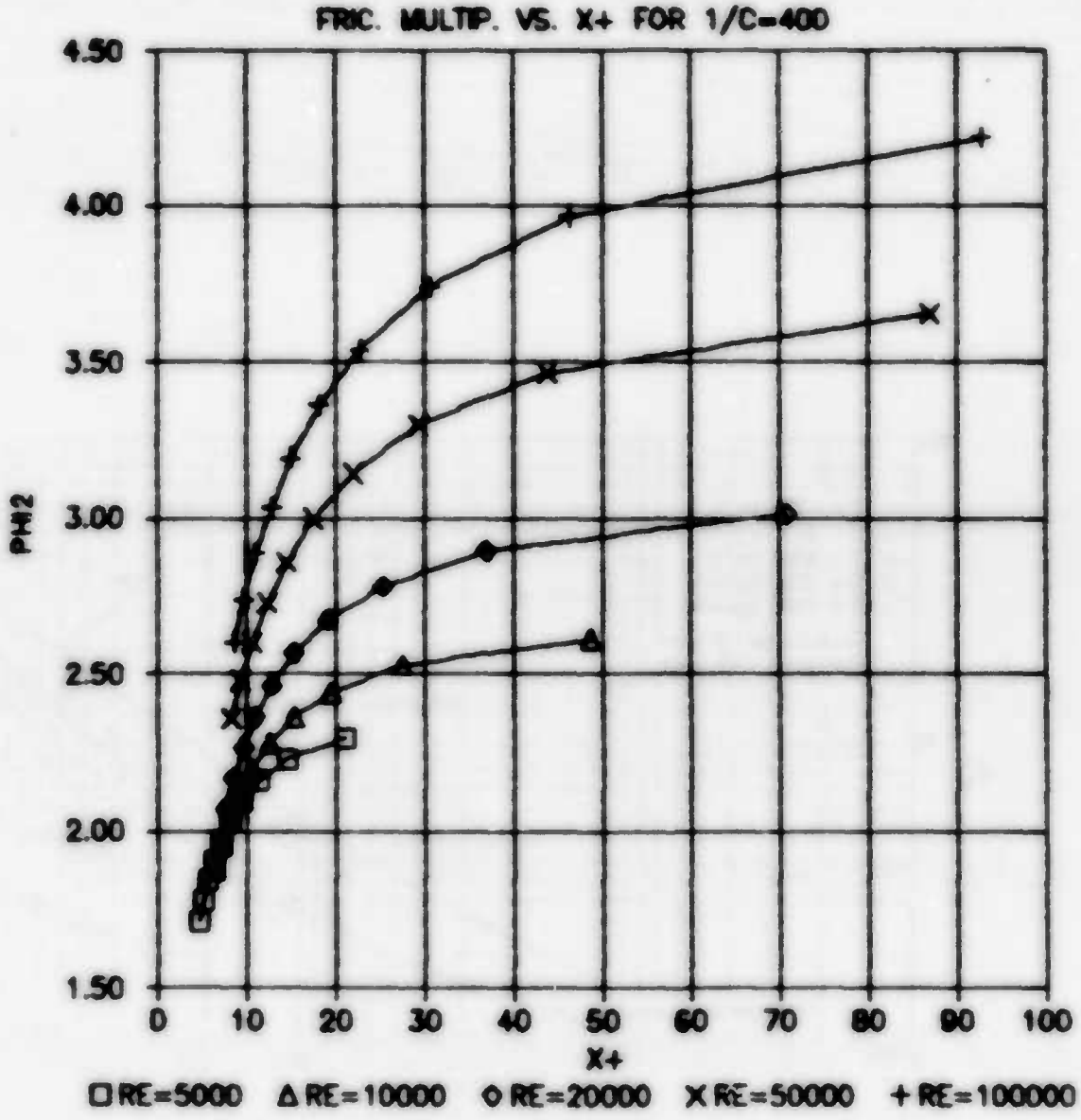

Figure 3.12. Two-Phase Friction Multiplier vs. Modified Flow Quality for C = 1/400

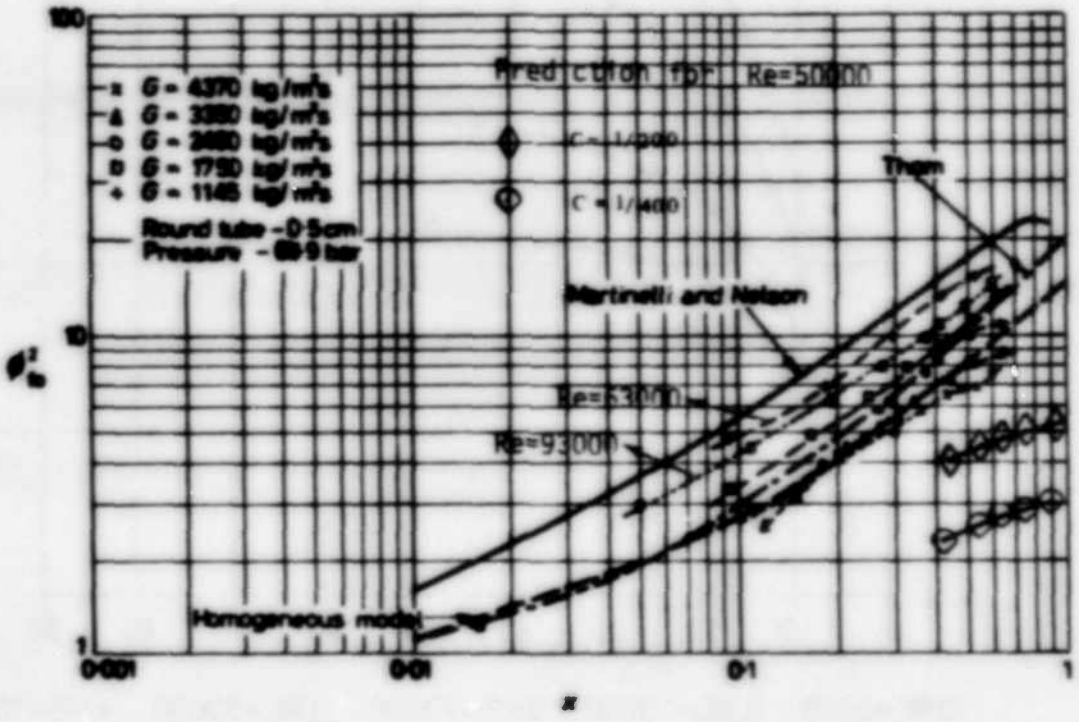

Fig. 3.13 - Comparison of the Predictions with Earth Gravity Two-Phase Friction Multiplier.

Section 4

TWO-PHASE HEAT TRANSFER COEFFICIENT

As discussed in Section 2, the two-phase heat transfer coefficient at earth gravity depends on the flow regime and whether the bulk liquid is subcooled or saturated. The heat transfer regimes for forced convective boiling are shown in Figure 4.1. The boundaries of the saturated forced convective boiling are shown in Figure 4.2. The present analysis is for saturated two-phase heat transfer which covers the nucleate boiling regime (regions C and D in Figure 4.1) and the forced convective regime (regions E and F in Figure 4.1) where there is no nucleation at the wall. As shown in Figure 4.2, the forced convective boiling can occur at any flow pattern, but normally at earth gravity this heat transfer regime occurs with the annular flow.

The majority of the existing correlations (30) and (31) are of the form

$$h_{TP} = h_{fo} f(X_{tt})$$

where h_{TP} and h_{fo} are the two-phase and single-phase liquid heat transfer coefficients, respectively, and X_{tt} is Martinelli parameter. These correlations have been developed for the forced convective region and have been modified for the application to saturated nucleate boiling regime. The Chen (32) correlation, however, is applicable to both regimes and has been developed by adding the contribution due to both mechanisms of heat transfer.

The present analysis should basically be valid to any mode of heat transfer which is controlled by the temperature difference in a narrow region close to the wall. However, because the velocity and density distributions developed in the previous section are used, the analysis

is valid for no vapor bubble at the wall. This will cover heat transfer for two-phase, two-component flow and single-component forced convection regime with bubbles within the liquid film or for nucleate boiling with a small number of nucleation sites, where fluid density at the wall can be approximated by the liquid density.

4.1 GOVERNING EQUATIONS

The conservation of energy for a two-dimensional channel is given by

$$\rho c_p \left(u \frac{\partial T}{\partial x} + V \frac{\partial T}{\partial y}\right) = \frac{\partial}{\partial y}\left(K \frac{\partial T}{\partial y}\right) + u \frac{dp}{dx} + \mu\phi \qquad (4\text{-}1)$$

where ϕ is the dissipation term. Following the same approach as in the previous section, it can be assumed that for the two-phase turbulent flow, the temperature consists of an average and a fluctuating component, i.e.,

$$T = \bar{T} + T'$$

Using the averaging rules shown in Section 2 and taking the time average of equation (4-1), we will get

$$c_p \bar{\rho}\,\bar{u} \frac{\partial \bar{T}}{\partial x} + c_p \bar{\rho}\,\bar{v} \frac{\partial \bar{T}}{\partial y} = \frac{\partial}{\partial y}\left(K \frac{\partial \bar{T}}{\partial y}\right) - c_p \overline{\rho' v'} \frac{\partial \bar{T}}{\partial y} - \frac{\partial}{\partial y}\left(c_p \bar{\rho}\, \overline{v'T'}\right)$$

$$+ \bar{u} \frac{d\bar{p}}{dx} + \overline{\mu\phi}$$

If it is assumed that the specific heat does not vary with y, the above equation reduces to

$$c_p \bar{\rho}\,\bar{u}\frac{\partial \bar{T}}{\partial x} + c_p \bar{\rho}\,\bar{v}\frac{\partial \bar{T}}{\partial y} = \frac{\partial}{\partial y}\left(K\frac{\partial \bar{T}}{\partial y}\right) - c_p\,\overline{\rho' v'}\frac{\partial \bar{T}}{\partial y} - \frac{\partial}{\partial y}\left(\bar{\rho}\,\overline{v'T'}\right)$$

$$+ \bar{u}\frac{d\bar{p}}{dx} + \overline{\mu\phi} \qquad (4\text{-}2)$$

In the compressible flow literature, the term $- c_p\,\overline{\rho' v'}\,\partial\bar{T}/\partial y$ in the above equation is combined with the transverse convective term to get

$$c_p \bar{\rho}\,\bar{u}\frac{\partial \bar{T}}{\partial x} + c_p \overline{\rho v}\frac{\partial \bar{T}}{\partial y} = -\frac{\partial q}{\partial y} + \frac{d\bar{p}}{\partial x} + \overline{\mu\phi} \qquad (4\text{-}3)$$

where in comparison to laminar energy equation

$$q = q_{Laminar} + q_{turbulent}$$

$$q = -K\frac{\partial \bar{T}}{\partial y} + c_p \bar{\rho}\,\overline{v'T'} \qquad (4\text{-}4)$$

The above definition for the heat flux is equivalent to assuming

$$\overline{\rho' v'}\,\bar{T} << \overline{v'T'}\,\bar{\rho} \qquad (4\text{-}5)$$

in equation (4-2) and defining (4-4) by comparing (4-2) to laminar energy equation.

In the superheated region near the wall, it is assumed that

$$q = q_w$$

$$\overline{v'T'} = -C\,\bar{v}'\,\bar{T}'$$

Applying the mixing length theory and using equal mixing lengths for the momentum and heat transfer, we will get

$$q_w = -K \frac{\partial \bar{T}}{\partial y} - c_p H^2 y^2 \left[1 - e^{-\frac{y}{F}} \right]^2 \rho \frac{\partial \bar{u}}{\partial y} \frac{\partial \bar{T}}{\partial y} \qquad (4\text{-}5)$$

4.2 NON-DIMENSIONAL EQUATIONS AND METHOD OF SOLUTION

Equation (4-5) is non-dimensionalized using the definitions of equation (3-23) and

$$T^+ = \frac{c_p \rho_L \sqrt{\frac{\tau_w}{\rho_L}}}{q_w} (T_w - T) \qquad (4\text{-}6)$$

If we drop the bar convention representing the mean component of the flow, (4-5) reduces to

$$\frac{dT^+}{dy^+} = \frac{1}{H^2 y^2 \left[1 - e^{-\frac{y^+}{F^+}} \right]^2 \rho^+ \frac{du^+}{dy^+} + \frac{1}{Pr}} \qquad (4\text{-}7)$$

It is known that the two-phase Prandtl number can be approximated by the value corresponding to the liquid, i.e.,

$$Pr = Pr_L$$

Equation (4-7) can be integrated along with the differential equations for ρ^+ and u^+ given by (3-28) and (3-29) for $y^+ < \delta^+$ and equations (3-24) and (3-25) for $y^+ > \delta^+$. Therefore, for a given value of the constant c, the state variable T^+ will be calculated as a function of y^+ and $\rho_c{}^+$.

In order to calculate the heat transfer coefficient, a mixed mean temperature is defined as follows

$$G A c_p T_m = \int \rho u c_p T \, d_A \tag{4-8}$$

For constant c_p, we will have

$$T_m = \frac{2 \int_0^R \rho u T (R-y) \, dy}{GR^2} \tag{4-9}$$

Non-dimensionalizing (4-9) and defining a heat transfer coefficient as

$$h = \frac{q_w}{T_w - T_m} \tag{4-10}$$

will result in

$$T_m = T_w - \frac{h (T_w - T_m)}{c_p G} \left[\frac{2}{R^{+2}} \int_0^{R^+} \rho^+ u^+ T^+ (R^+ - y^+) \, dy^+ \right]$$

$$h = \frac{c_p G}{\frac{2}{R^{+2}} \int_0^{R^+} \rho^+ u^+ T^+ (R^+ - y^+) \, dy^+} \tag{4-11}$$

Nusselt number is defined as

$$Nu = \frac{2\,R\,h}{K} = \frac{Re\,Pr}{\frac{2}{R^+}\int_0^{R^+} \rho^+ u^+ T^+ (R^+ - y^+)\,dy^+} \qquad (4\text{-}12)$$

The method of solution consists of integrating (4-7) along with equations (3-28) and (3-29) for $y^+ < \delta^+$ and equations (3-25) and (3-26) for $y^+ > \delta^+$. At every step the integral in equation (4-12) is performed and a Nusselt number is calculated. All the solutions are performed for $Pr_L = 1.0$ in the present analysis.

The computer program ZROG, discussed earlier, actually solves the system of three differential equations for the state variables u^+, ρ^+, and T^+.

4.3 RESULTS AND DISCUSSION

Temperature distributions for a given value of the center line density ($\rho_c^+ = 0.1$) and different values of c are shown in Figure 4.3. The change in the slope in this figure at around $y^+ = 10$ is not really predicted by the model. This is due to logarithmic scales, the few available points between $y^+ = 0$ and 10, and the method of plotting. However, the change in slope and increase in temperature at larger values of y^+ (e.g., $y^+ = 100$ for $c = 1/400$) is representative of the true phenomenon. This rise in temperature at larger y^+ is due to increased void within the flow. Figures 4.4 and 4.5 show the temperature distribution for $c = 1/200$ and $1/400$ and different values of the center line density.

The Nusselt number predicted by equation (4-12) is not a function of Re and Pr_L alone, and it varies with the center line density. Similar solutions for the single-phase turbulent flow in a pipe express Nu in

terms of Re and Pr alone. The reason for this is that, in addition to the differential method as described for the two-phase flow above, the single-phase models assume a velocity profile to calculate the state variables at the tube center line.

The Nusselt numbers for c = 1/200 and 1/400 for different Re and ρ_c^+ are shown in Tables 4-1 and 4-2. It can be seen that Nu increases with Re as expected. Nu decreases with increasing center line density but reverses this trend at certain Reynolds numbers. The reason for this reversal in the trend needs to be investigated.

Table 4.1 - Nusselt Number as a Function of Reynolds Number and Center Line Density for C=1/200 and Pr=1.0

	Nu					
	Re					
ρ_c^*	3000	5000	7000	10000	20000	50000
0.01	37.47	57.32	70.64	82.57	108.60	156.70
0.02	36.83	56.14	68.15	81.92	112.30	179.40
0.03	36.06	53.56	66.31	80.54	115.20	190.60
0.04	35.31	52.11	64.71	79.20	115.80	196.80
0.05	34.59	50.80	63.24	77.99	115.90	199.90
0.06	34.02	49.59	61.87	76.66	114.90	201.50
0.07	33.48	48.56	60.56	75.30	114.10	202.20
0.08	32.68	47.49	59.30	73.94	113.00	200.20
0.09	32.17	46.46	58.09	72.58	111.70	201.60
0.10	31.55	45.49	56.92	71.64	110.30	200.10

Table 4.2 - Nusselt Number as a Function of Reynolds Number and Center Line Density for C=1/400 and Pr=1.0

	Nu					
	Re					
Rho_c^+	5000	7000	10000	20000	50000	100000
0.01	46.41	63.02	85.43	124.10	170.00	229.80
0.02	45.52	61.83	82.38	123.30	186.50	266.20
0.03	44.65	60.69	79.96	121.90	194.30	284.80
0.04	44.60	59.59	78.43	120.60	197.80	295.90
0.05	43.73	57.80	76.48	118.70	199.70	302.80
0.06	42.87	56.79	74.65	116.80	199.60	306.70
0.07	42.02	55.82	72.92	114.90	199.20	308.60
0.08	41.98	54.88	71.87	113.30	198.20	309.40
0.09	41.14	53.97	70.27	111.30	196.70	309.10
0.10	30.31	52.37	68.73	109.30	194.80	307.90

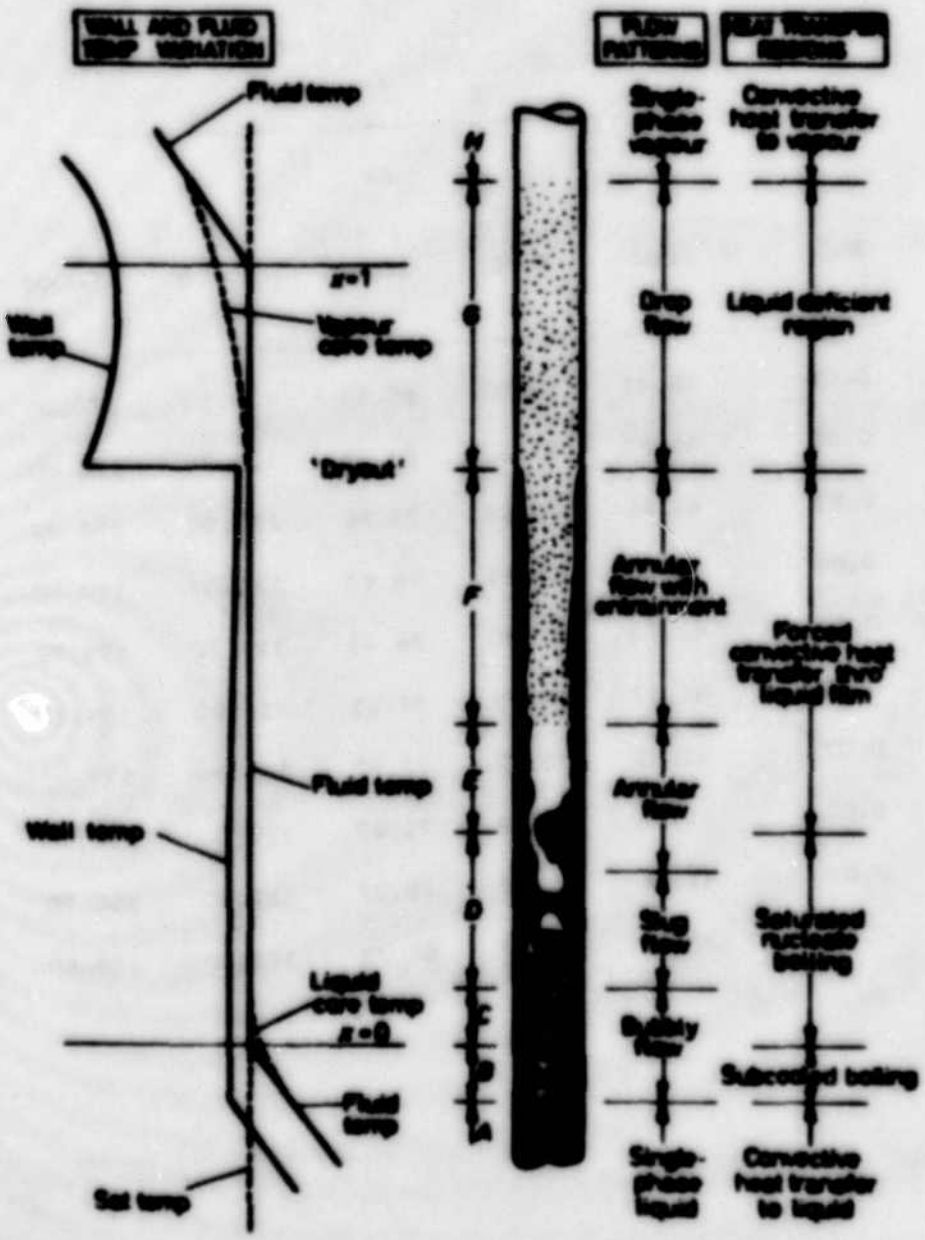

Fig. 4.1 Regions of Heat Transfer in Convective Boiling

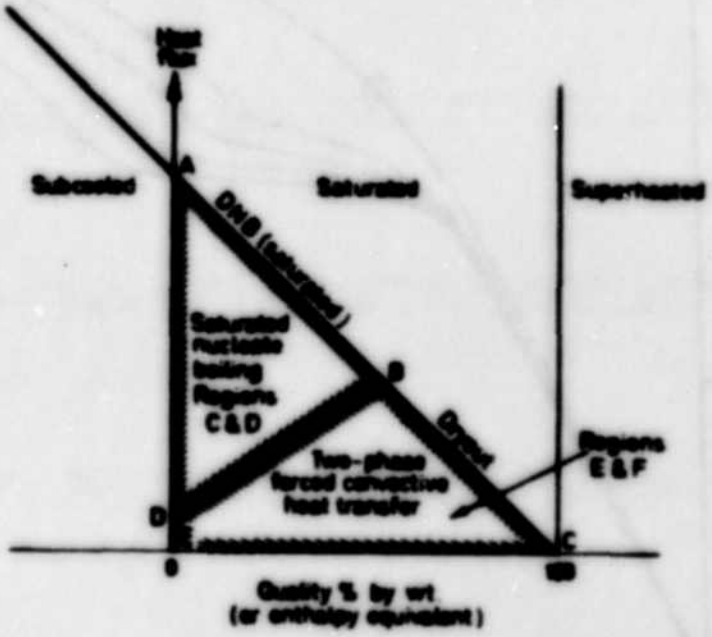

Fig. 4.2 Boundaries of Saturated Forced Convective Boiling

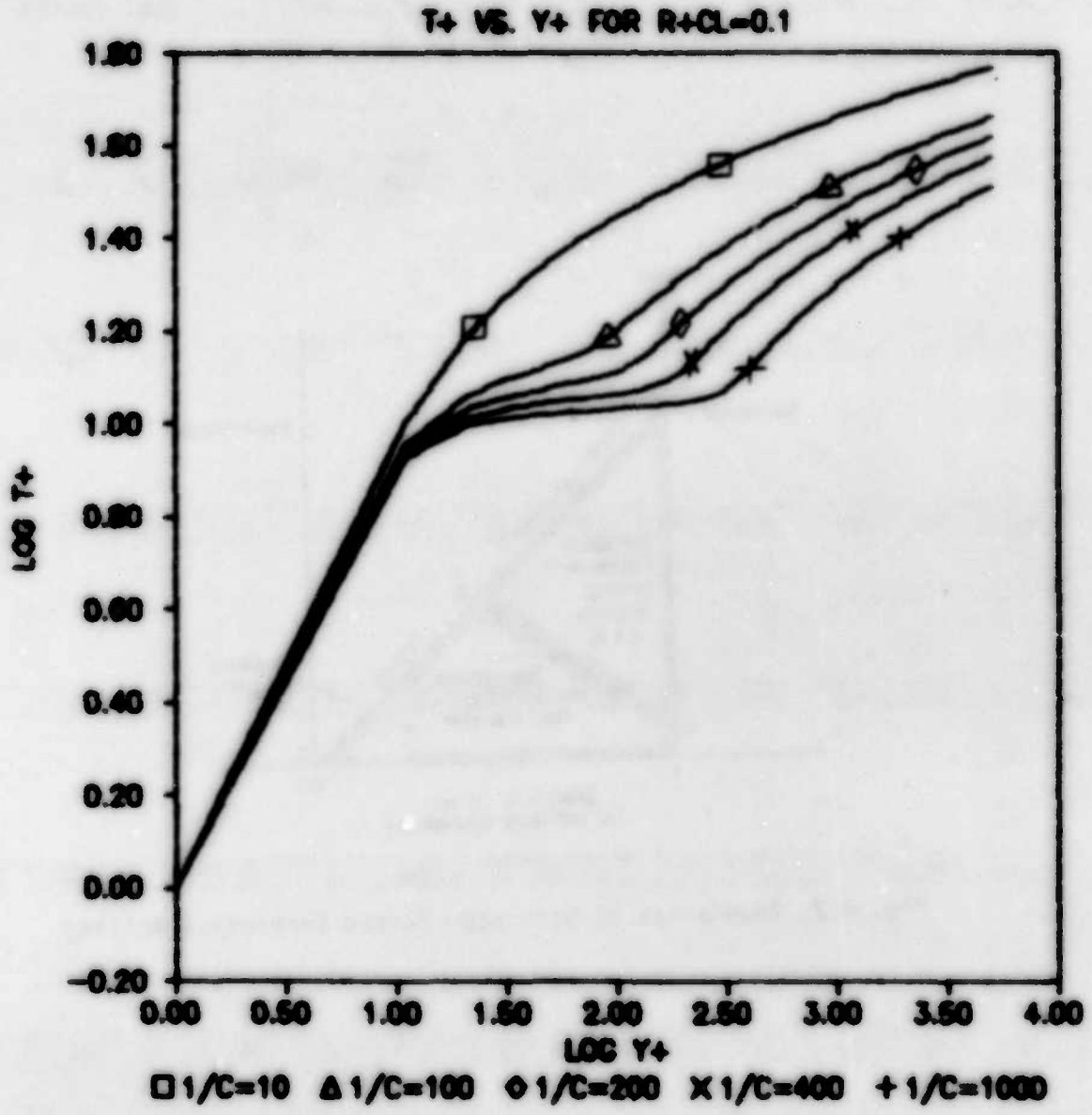

Figure 4.3. Effect of the Parameter c on the Temperature Profile for $\rho_c^+ = 0.1$

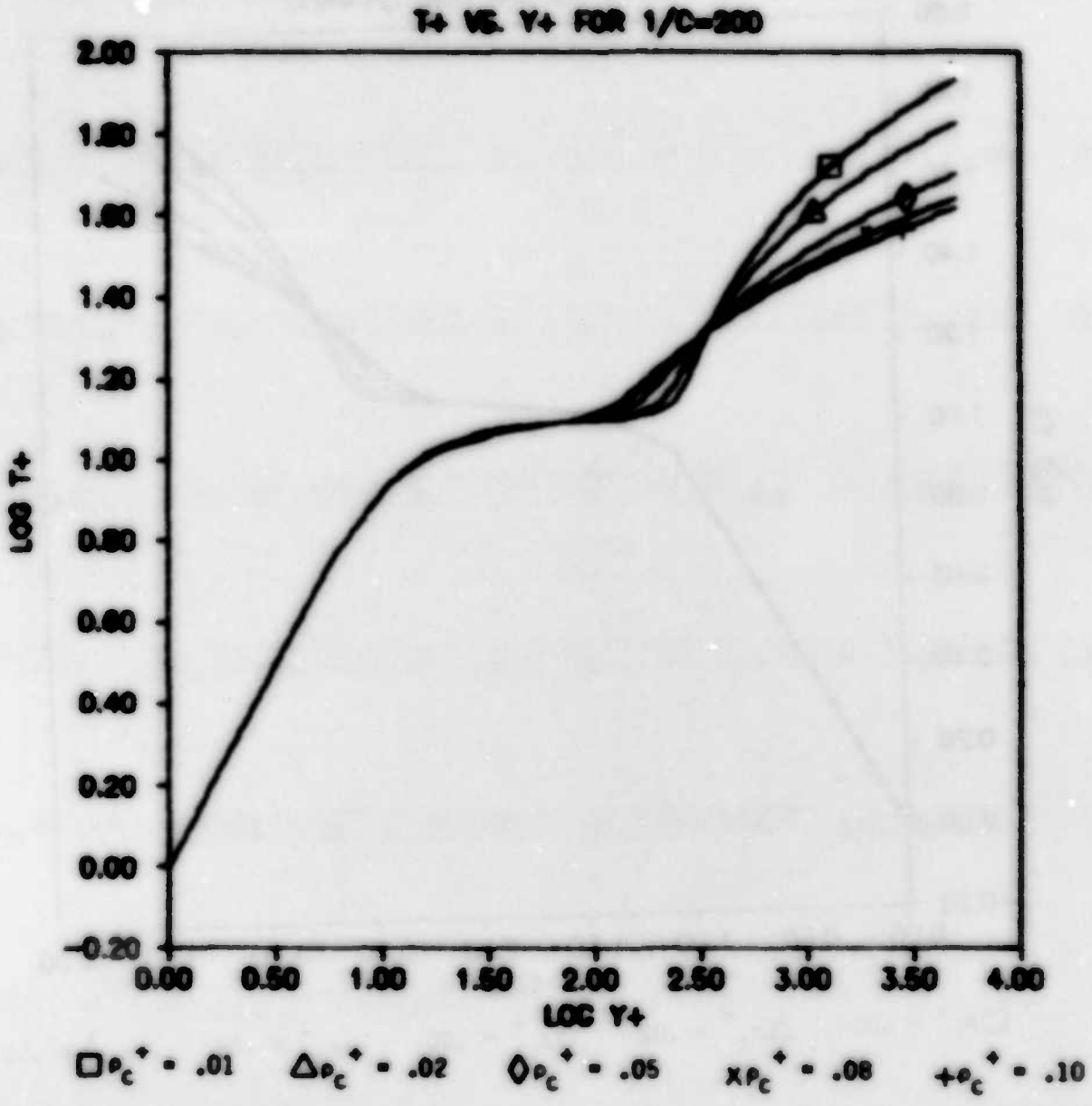

Figure 4.4. Effect of the Center Line Density on Temperature Profile for c = 1/200

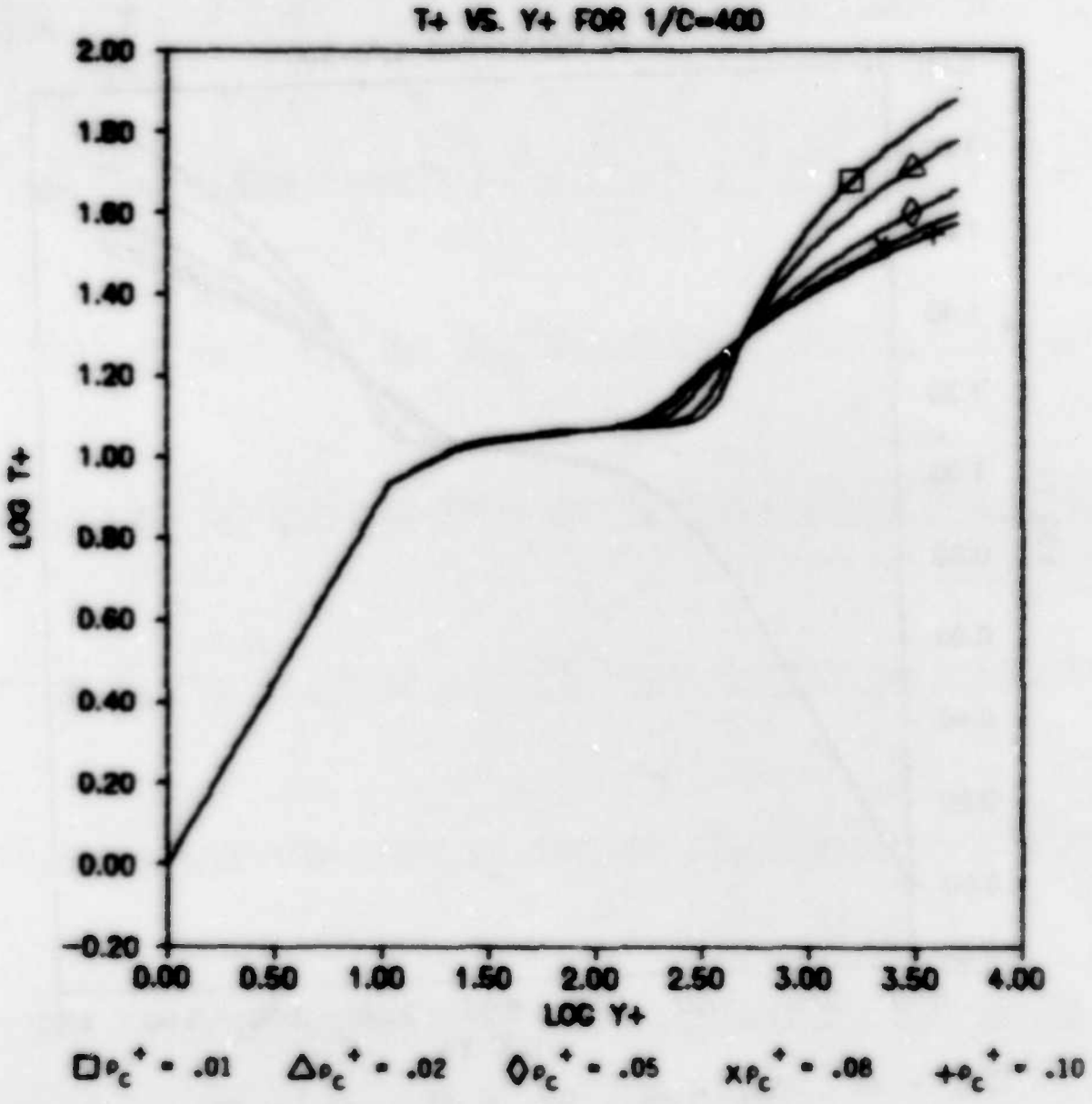

Figure 4.5. Effect of the Center Line Density on Temperature Profile for c = 1/400

Section 5

CONCLUSIONS AND RECOMMENDATIONS

Turbulent mixing length theory was used to develop models for two-phase friction multiplier, void-quality relation, and two-phase heat transfer coefficient under zero or negligible gravity. Differential method of approach was used to solve the governing equations for the conservation of mass, momentum, and energy. The mixing length model of Van Driest (24) was used here, and a sublayer region was considered to avoid discontinuity in the numerical solution. The non-dimensional velocity, density, and temperature were used to solve for the desired variables. This model contains a free parameter, c, which ideally should be determined from experimental results.

In this analysis, the flow was assumed to be locally homogeneous, but the void distribution was allowed to vary within the channel cross section. The driving force for this distribution is a lift force which acts on the bubbles and drives them to the region of higher velocity. Physically, this model predicts the correct trends for the two-phase flow. As the Reynolds number increases:

- The bubbles will be more uniformly distributed and the flow becomes more homogeneous.
- The void fraction increases and the distribution approaches the homogeneous distribution.
- The two-phase friction factor, $\phi_o^2 f_o$, decreases.
- Nusselt number increases.

However, it is believed that the values for c used in the predictions are too small and c on the order of 1/20 to 1/50 will be more

appropriate. This will result in two-phase multipliers larger than homogeneous which will approach homogeneous distribution as Reynolds number is increased.

The Nusselt number predicted by this model is a function of Reynolds number, Prandtl number, and the velocity and density distributions which are specified through the center line density. The predicted Nusselt numbers reverse their dependence on center line density at a specific Reynolds number, as shown in Tables 4.1 and 4.2. This is related to the temperature distribution as shown in Figures 4.3 to 4.5.

Certain trends predicted by this model need to be investigated further to establish the theoretical bases of the model. These are:

1. The predictions should be performed for larger values of c (1/20 to 1/100) and the results compared to homogeneous distribution as flow velocity increases.

2. The assumption of $\tau = \tau_w$ and $q = q_w$ should be evaluated, and the possibility of including the exact relations

$$\tau = \tau_w \left(1 - \frac{Y}{R}\right) \qquad q = q_w \left(1 - \frac{Y}{R}\right)$$

should be investigated.

3. The void-quality and two-phase multiplier should be compared to more earth gravity data.

4. The temperature profile and its dependence on center density should be studied.

5. The effect of Prandtl number on temperature distribution and Nusselt number should be investigated.

6. Nucleation at the wall was neglected in the present model. The possibility of extending the model to include nucleation needs to be investigated.

The free parameter in the present model needs to be specified more accurately. Obviously, experimental results under reduced gravity or conditions which simulate the flow behavior at zero gravity are the ultimate test of the model. These types of tests should be considered in the future, and they can be used to establish the parameter c. In the absence of such experiments, high pressure two-phase flow test results can be used for better estimation of c. An alternative approach should also be considered which consists of selecting a constant sublayer length and allowing the model to calculate c, velocity, density, and temperature distributions. A series of two-phase flow tests have been designed and planned for the future space shuttle flights (36). The design for these experiments is based on earth gravity models. It will be very beneficial to review these designs in view of the predictions by the present model and also study the possibility of enhancing these tests to calculate the parameters needed for this model, which seems to be the only one for zero gravity.

In addition to the above recommendations, which are mainly for establishing the present approach, efforts are needed to study the flow regime transitions at zero gravity and also other possible two-phase flow and heat transfer regimes.

Section 6

REFERENCES

1. T. Mahefkey, "Military Spacecraft Thermal Management: The Evolving Requirements and Challenges," AIAA Paper 82-0827, June 1982.

2. R. E. Eastman et al., "Two-Phase Fluid Thermal Transport for Spacecraft," AFWAL Report No. AFWAL-TR-84-3028, October 1984.

3. R. Siegel, "Effects of Reduced Gravity on Heat Transfer," Advances in Heat Transfer, Vol. 4, 1967.

4. S. S. Papell and O. C. Faber, "Zero and Reduced Gravity Simulation on a Magnetic-Coiled Pool-Boiling System," NASA TN D-3288, February 1966.

5. Y. A. Kirichenko and A. I. Charkin, "Studies of Liquid Boiling in Imitated Reduced Gravity Fields," 4th International Heat Transfer Conference, Versailles, France, September, 1970.

6. G. Malcotsis, "The Mechanism of Bubble Detachment from a Wall at Zero and Negative Gravity," J. Fluid Mech., Vol. 77, 1976.

7. N. Bakhru and J. H. Lienhard, "Boiling from Small Cylinders," Int. J. Heat Mass Transfer, Vol. 15, 1972.

8. J. T. Congelliere et al., "The Zero G Flow Loop: Steady-Flow, Zero Gravity Simulation for Investigation of Two-Phase Flow," Advances in Astronautical Sciences, Vol. 14, 1963.

9. J. C. Feldmanis, "Pressure and Temperature Changes in Closed Loop Forced Convection Boiling and Condensing Processes Under Zero Gravity Conditions," Proc. Inst. Environ. Sci., April 1966.

10. D. B. Heppner, et al., "Zero-G Experiments in Two-Phase Fluid Flow Regimes," ASME Paper 75-ENAS-24, 1975.

11. T. H. Cochran et al., "Forced Convection Peak Heat Flux on Cylindrical Heaters in Water and Refrigerant 113," NASA TN D-7553, February 1974.

12. T. H. Cochran et al., "Forced Convection Boiling Near Inception in Zero Gravity," NASA TN D-5612, January 1970.

13. S. S. Papell et al., "Buoyancy Effects on Critical Heat Flux of Forced Convective Boiling in Vertical Flow," NASA TN D-3672, October 1966.

14. A. A. Fowle et al., "A Pumped, Two-Phase Flow Heat Transport System for Orbiting Instrument Payload," AIAA 16th Thermophysics Conference, June 1981, AIAA-81-1075.

15. S. Ollendorf, F. A. Costello, "A Pumped Two-Phase Cooling System for Spacecraft," 13th Intersociety Conference on Environmental Systems, July 1983, SAE 831099.

16. H. Merte, "Incipient and Steady-State Boiling of Liquid Nitrogen and Liquid Hydrogen Under Reduced Gravity," NASA-20228, November 1970.

17. E. G. Keshock and R. Siegel, "Forces Acting on Bubbles in Nucleate Pool Boiling," NASA TN D-2299, 1964.

18. R. Siegel and E. G. Keshock, "Effects of Reduced Gravity on Nucleate Boiling Under Normal and Reduced Gravity Conditions," AICHE J., Vol. 10, No. 4, 1964.

19. S. G. Bankoff, "A Variable Density Single-Fluid Model of Two-Phase Flow with Particular Reference to Steam-Water Flow," J. Heat Transfer, Series C.82, 1960.

20. N. Zuber and J. Findlay, "Average Volumetric Concentration in Two-Phase Flow Systems," J. Heat Transfer, 87, 453, 1965.

21. S. Levy, "Prediction of Two-Phase Pressure Drop and Density Distribution from Mixing Length Theory," J. Heat Transfer, 85C, 1963.

22. H. Schlichting, Boundary Layer Theory, 6th Edition, McGraw-Hill, 1968.

23. F. M. White, Viscuous Fluid Flow, McGraw-Hill, 1974.

24. E. R. Van Driest, "On Turbulent Flow Near a Wall," Heat Trans. Fluid Mech. Inst., 1955.

25. R. Clift et al., Bubbles, Drops, and Particles, Academic Press, 1978.

26. S. I. Rubinow and J. B. Keller, "The Transverse Force on a Spinning Sphere Moving in a Viscuous Fluid," J. Fluid Mech., 11, 1961.

27. P. G. Saffman, "The Lift on a Small Sphere in a Slow Shear Flow," J. Fluid Mech., 22, 1968.

28. G. Kocamustafaogullari et al., "Unified Theory for Predicting Maximum Fluid Particle Size for Drops and Bubbles," NUREG/CR-4028, ANL-84-67, October 1984.

29. J. G. Collier, Convective Boiling and Condensation, McGraw-Hill, 1972.

30. C. E. Dengler, J. N. Addoms, "Heat Transfer Mechanism for Vaporization of Water in Vertical Tube," Chem. Eng. Progress Symp. Series, Vol. 52(18), 1956.

31. S. A. Guerrieri, R. D. Talty, "A Study of Heat Transfer to Organic Liquids in Single Tube, Natural Circulation Vertical Tube Boilers," Chem. Eng. Progress Symp. Series, Vol. 52(18), 1956.

32. J. C. Chen, "A Correlation for Boiling Heat Transfer to Saturated Fluids in Convective Flow," 6th National Heat Transfer Conf., ASME 63-HT-34, 1963.

33. D. C. Hustvedt and R. L. Oonk, "Preliminary Design of Flight Hardware for Two-Phase Fluid Research," NASA CR-168072, February 1982.

*U.S. Government Printing Office: 1985 — 559-065/20011

END

FILMED

8-85

DTIC